THEORETICA CHIMICA ACTA

Theor Chim Acta (1985) 68: 471-506

Electron difference densities and chemical bonding

W. H. Eugen Schwarz*, Petros Valtazanos, and Klaus Ruedenberg

Ames Laboratory, USDOE, and Department of Chemistry, Iowa State University, Ames, IA 50011, USA

(Received July 12/Accepted September 2, 1985)

In view of recent advances in X-ray technology it may be possible to deduce information regarding chemical bonding from experimentally determined electron densities. The construction of difference density maps represents a possible intermediate step in attaining this goal, but unresolved questions exist regarding appropriate definitions and interpretations of such maps. To shed light on these problems, theoretical difference densities are determined by ab-initio calculations for the molecules H_2, He_2, Li_2, Be_2, N_2 and F_2 at various internuclear distances. An examination of these difference density maps shows that the identification of those features of molecular electronic densities which are related to chemical bonding requires a judicious construction and a careful analysis of difference densities between molecules and their constituent atoms. Chemically relevant deformations can be small compared to density differences between different components of degenerate atomic groundstates and, consequently, chemical information can be swamped when difference densities are formed with spherically averaged atoms. To avoid such artifacts, oriented unaveraged atomic states must be subtracted for the formation of meaningful Chemical Difference Densities. The latter are explainable by means of a partitioning in terms of contributions from non-bonded inner shells, from lone pairs and from sigma and pi bonding shells. Such partitionings can be obtained through decompositions in terms of natural orbitals from correlated wavefunctions. Canonical SCF orbitals prove to be considerably less effective. Internuclear distances are found to have a great influence upon difference densities regardless of the attractive or repulsive nature of the interactions.

* *Permanent address:* Theoretical Chemistry Group, FB 8, The University, POB 10 12 40, D-5900 Siegen, Federal Republic of Germany

1. Introduction

Recent advances in X-ray techniques have made it possible to determine molecular electron densities so accurately that, at least for the lighter elements, the remaining margin of error is smaller than those changes in electron densities which are believed to occur when chemical bonds are formed [1–5]. Experimentalists have therefore expressed the hope of being able to measure features of molecular electron densities which would permit inferences to be drawn regarding characteristics of chemical bonding.

This objective cannot be achieved by a mere examination of raw molecular densities. One reasonable approach consists of studying differences between molecular and atomic densities, the so-called *difference densities* (DD's) [6a]. In the implementation of such a program the question arises which atomic densities should be subtracted from the molecular density to form suitable DD's. There is no way of observing the densities of atoms in a molecule as distinct from the molecular density. In fact, so far it has not even been possible to measure electron densities of free atoms except for some noble gases. Atomic densities can however be calculated theoretically with considerable accuracy and experimentalists have therefore used theoretically determined atomic densities in combination with experimentally determined molecular densities to form difference densities. But even so, there remain questions.

For one thing, there are many ways of fitting an atom into a molecule. Theorists have long been familiar with the fact that it is by no means trivial to deduce appropriate "atoms in molecules" from molecular electronic wavefunctions and it stands to reason that similar problems are encountered in the selection of those "promolecules" which are most suitable for constructing meaningful difference densities. Any *arbitrary* convention regarding standard reference densities would seem inadequate for insuring that the resulting difference densities make significant information manifest.

For another thing, it is not at all obvious what physical inferences can in fact be drawn from difference densities. Since electron densities have an almost immediate conceptual appeal [6b], there seems to exist a widespread expectation that illuminating insights can be obtained in an uncomplicated and straightforward manner by "common sense" reasoning. Unfortunately such is not the case and it has proven to be difficult to establish physical or chemical interpretations for the features found on DD maps.

Fortunately, quantum chemical methods, too, have made noteworthy strides in the past decades and densities can now be calculated for many molecules with a high degree of accuracy [2]. It is therefore possible to compute difference densities theoretically and thereby to investigate which DD formulations are apt to yield chemical information and what can be learned from them. It would seem likely that such an approach, when pursued with care, can yield answers which would be difficult to obtain in other ways and that knowledge regarding chemical bonding will be gained more readily when the methodological sophistication in contemporary experimental technology and in the mathematical deduction of

electron densities from X-ray measurements is matched by a corresponding sophistication in relating the resulting information to quantum chemical theory of a sufficient degree of accuracy.

It is the intent of the present investigation to contribute towards such a synthesis by analyzing theoretically calculated difference densities for a number of diatomic molecules in greater depth than has been done in the past. It proves possible to sort out characteristic bonding and non-bonding DD contributions by employing oriented ground state atoms as reference densities (instead of the conventional spherically averaged ones) to form DD's, by using natural orbitals of correlated wavefunctions (rather than the commonly used canonical SCF MO's) to decompose the total densities, by relating the behavior of the valence electrons to the shapes and the interaction ranges of the effective core potentials acting on them, and by understanding density changes in terms of orbital interferences, orbital contractions and non-bonded repulsions. The variations of DD's with internuclear distances also disclose valuable information.

The methods used to calculate the atomic and molecular wavefunctions are described in Sect. 2. In Sect. 3, certain elementary features of difference densities are discussed pertaining to bonding electrons, to non-bonding electrons and to the effect of inner cores. In this context the molecules H_2, He_2, Li_2, and Be_2 are considered. In Sect. 4, the difference density of F_2 is examined in considerable detail. In Sect. 5, the difference density of N_2 is analyzed. The conclusions and inferences which we draw from these studies are summarized in Sect. 6.

2. Description of method

The results reported here are obtained by FORS calculations. The FORS method [7a] is an MCSCF approach where the *number of configuration-generating orbitals* (CGO's) in each irreducible representation of the relevant symmetry group is chosen to be equal to the *number* of minimal-basis-set atomic orbitals in that irrep. *All* configurations that can be generated from these CGO's and that are compatible with the geometric and spin symmetry of the desired state are included in the CI expansion, except that the inner orbitals remain always doubly occupied. This set of configurations spans a Full Reaction Space. The configuration mixing coefficients as well as the orbital shapes are then optimized simultaneously by an MCSCF procedure and the resulting configuration space is then called the *Full Optimized Reaction Space* (FORS). The FORS model is "size consistent" and, in contrast to the SCF approximation, allows for proper dissociation, a feature which is essential for the present investigation.

An important feature of the full configuration space is its invariance under non-singular transformations among the optimal CGO's (i.e. while the individual configurations generated from the transformed CGO's are different, the configuration space spanned by all of them is identical to the one spanned by the original CGO's). Hence, the molecular wavefunctions and energies are the same regardless of whether the original or the transformed CGO's are used. For this reason a FORS wavefunction can also be visualized by the following model. The *full*

valence configuration space is generated from the *minimal-basis-set* atomic orbitals of the atoms in the molecule. The best wavefunction in this "Full Reaction Space" is then found, where moreover *the minimal basis set AO's are allowed to deform for optimal adaptation to the molecular surroundings.*

This adaptation is achieved by the orbital optimization implicit in the MCSCF process and requires the expansion of the configuration generating orbitals in terms of an extended set of atomic orbital basis functions. The extended bases used here consist of even-tempered gaussion primitives contracted in Raffenetti-type fashion [8]. Specifically the following bases are employed: (14s7p2d/4s3p2d) for the atoms F, N, Be; (12s3p/4s3p) for Li; (8s3p/4s3p) for helium; and (6s2p/2s2p) for hydrogen. For the isolated atoms, these extended bases yield the uncontracted (14s, 7p) SCF function in F, N, Be, and the uncontracted 12s, 8s and 6s wavefunctions in lithium, helium and hydrogen, respectively.

In the calculations for the He_2 system the full configuration space was furthermore enlarged by increasing the number of configuration generating orbitals from σ_g, σ_u (corresponding to the minimal basis set on each atom) to $1\sigma_g$, $2\sigma_g$, $3\sigma_g$, $1\sigma_u$, $2\sigma_u$, $3\sigma_u$, πx_g, πx_u, πy_g, πy_u (corresponding to the AO set $1s$, $2s$, $2p_x$, $2p_y$, $2p_z$ on each atom). These He_2 calculations were thus CASSCF [7b] calculations with 149 configurations (the corresponding calculations for the He atom had 5 configurations). In fact, the DD's reported in Fig. 1F-K come from these calculations. Within the resolution shown on these maps, the inclusion of this additional correlation had however no discernable effect on the DD's.

Selected energies resulting from various calculations are listed in Table 1.

Table 1. Atomic and molecular energies

Molecule	F_2	N_2	Be_2	Li_2	H_2
$R \approx$ Equilibrium[a]	2.68	2.06	4.50	5.00	1.40
E(SCF)[b]	−198.76401	−108.98731	−29.13160	−14.87074	−1.12873
E(FORS)[b]	−198.84432	−109.13441	−29.22107	−14.89821	−1.14677
2E(Atom, FORS)[b]	−198.81558	−108.80073	−29.23345	−14.86514	−0.99968
ΔE(SCF)[c]	1.40	−5.08	2.77	−0.15	−3.51
ΔE(FORS)[c]	−0.78	−9.08	0.34	−0.90	−4.00
ΔE(Exptl)[c]	−1.66	−9.91	−0.08[d]	−1.06	−4.75

Molecule	He_2	He_2	He_2	2He
R[a]	0.6	1.5	2.5	∞
E(SCF = FORS)	−3.44506	−5.37926	−5.68194	−5.72301
E(CASSCF)[b,e]	−3.53557	−5.45623	−5.75419	−5.79442
ΔE(SCF = FORS)[c]	62.00	9.36	1.12	—
ΔE(CASSCF)[c,e]	61.46	9.20	1.09	—

[a] In bohr
[b] In hartree
[c] Binding energy in eV
[d] Theoretical value, from [17]
[e] 149 configurations, see text

Because of the aforementioned invariance of the Full Optimized Reaction Space under orbital transformations, this configuration space can also be generated from the *natural orbitals* of the FORS wavefunction, the FORS-NO's. The latter have the great conceptual advantage that the total FORS density is simply the sum of the densities of the individual FORS-NO's, weighted with their occupation numbers. All orbital decompositions reported in the sequel are therefore based on FORS-NO's.

For the sake of comparison, single-configuration restricted HF-SCF calculations were also performed. In these cases, the orbital decompositions are based on the densities of the *canonical* SCF orbitals.

All plots exhibited in the subsequent sections represent DD's, i.e. differences of electron densities. They display contours DD = constant in planes containing the internuclear axis. *Thin lines represent positive DD values, dashed lines represent negative DD values and bold lines correspond to DD = 0. The increment between adjacent contours is* 0.04 *electron/bohr*^{3} = 0.27 *electron/*Å^3 *in all figures, with the exceptions of Figs.* 1 *and* 3 *where the increments are stated explicitly.* Since theory as well as good instruments under favorable conditions can yield electron densities in bond and lone-pair regions as accurate as about 0.01 electron/Å^3, the details shown in the plots are significant.

3. Elementary features of difference densities

A closer examination of difference densities in various molecules shows rather quickly that deeper insights are gained when the variation of the DD's with the geometric parameters is included in the analysis. In the subsequent sections we shall furthermore see that these variations can be explained through a decomposition of the total difference density in terms of suitable orbital contributions because the latter exhibit a simpler behavior. In the present section we discuss three elementary features which are important in this context. They are: (i) the difference density for two electrons (one on each atom) between which a bonding interaction develops; (ii) the difference density for two lone pairs (one on each atom) between which a nonbonded repulsion develops; (iii) the effect of atomic cores on difference densities.

3.1. The electron pair bond in H_2

The electron pair bond between singly occupied atomic orbitals is the most common covalent bond type by far and difference densities stemming from such bonds constitute essential contributions to the total difference densities of many molecules. The simplest prototype is found in the hydrogen molecule, and an examination of its difference density yields instructive insights, even though atoms from higher periods exhibit distinctive modifications.

Density difference maps of H_2 have been calculated and discussed in the literature for a number of approximations [9, 10]. Figure 1A–E exhibits DD maps of H_2 obtained from FORS calculations.

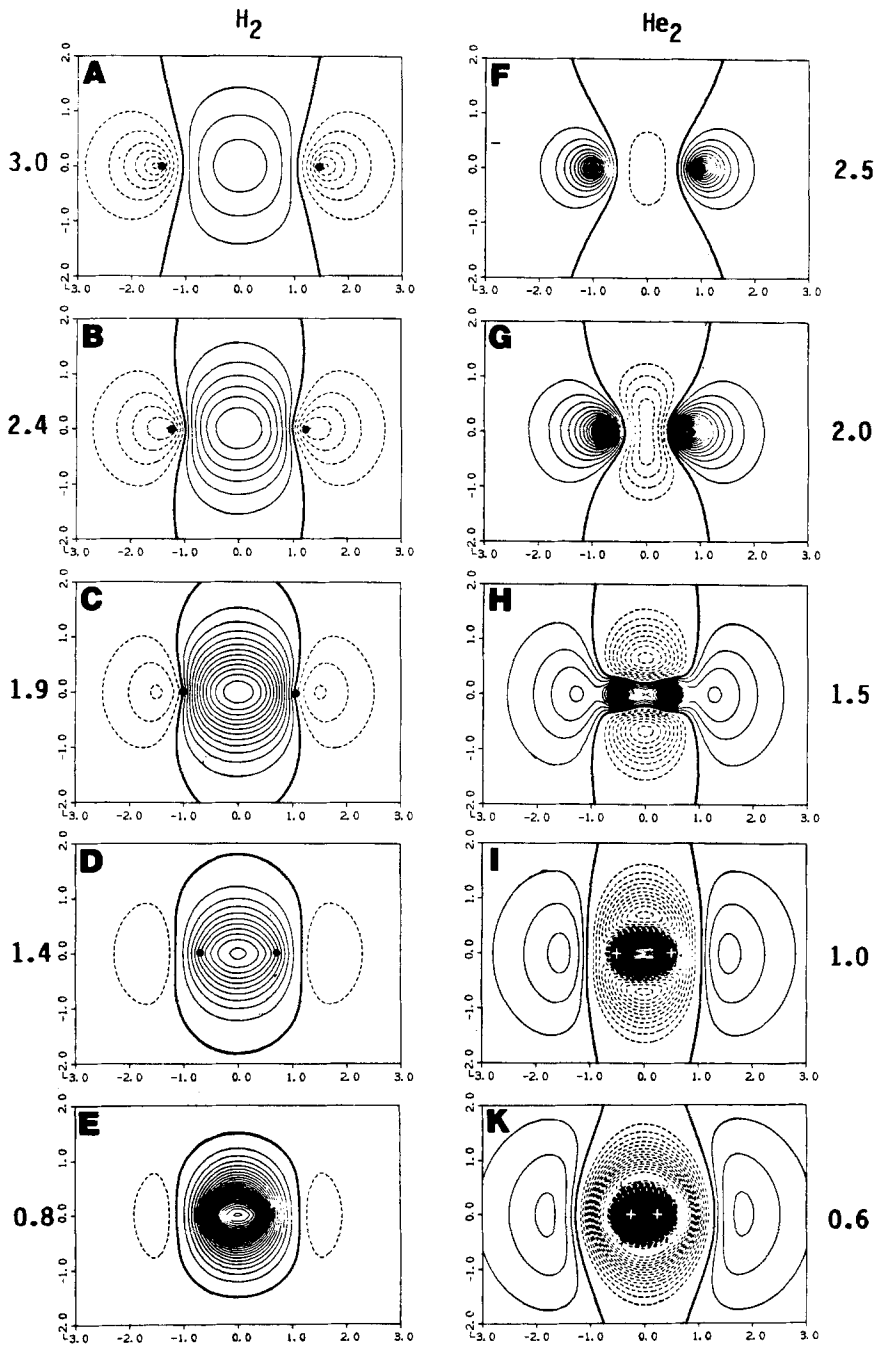

Fig. 1. Difference densities for H_2 (panels **A–E**) and He_2 (panels **F–K**). The internuclear distances (in units of a = one bohr) are indicated next to each panel. The increments between adjacent contours are 0.004 e/a^3 for panels **A**, **B**, **C** and for the negative contours on panels **D**, **E**. They are 0.01 e/a^3 for the positive contours on panels **D**, **E** and for all contours on panels **F–K**

At large distances (Fig. 1A), where the atomic orbitals are just beginning to overlap, the density increases at and around the bond center and it decreases at and around the nuclei, on the "bond side" as well as all the way on the side away from the bond. The DD describes therefore a population transfer *from* the region *around* the nuclei *towards* the bond *center*, and this charge shift is most easily described as the result of the *interference* of the practically *undeformed* atomic orbitals which are being superimposed. Such a modification of the atomic density *lowers* the *molecular* energy because it *lowers* the *kinetic* energy [10, 11]. There also occurs a concomitant interference *increase* of the *potential* energy, but it offsets the kinetic energy decrease only partially.

If this interference effect would remain dominant at shorter internuclear distances, then the region of charge accumulation (i.e. positive DD) would shrink correspondingly. Figure 1A–E shows however that, in fact, the extent of this region remains nearly unchanged in absolute value along the internuclear axis so that it appears as if the nuclei dive into this region of positive DD as they approach each other. This behavior of the DD is due to the fact that the atomic orbitals, while being superimposed, *contract* as the nuclei approach each other [10, 12]. The contractive effect modifies the interference effect to give the depicted DD's. In the lateral direction it manifestly leads to a contraction of the electron charge in the direction of the internuclear axis.

At medium distances (Fig. 1B–D) the atomic orbital contraction is best understood as a response which is triggered by the decrease of the local *kinetic energy density* (i.e. $\hbar^2|\nabla\psi|^2/2m$) in the central region. This is seen most easily at the equilibrium distance (Fig. 1D) because, there, the virial theorem must be rigorously satisfied in its simple form $E = -T = V/2$ and, in H_2, it applies entirely to the two bonding electrons. Without atomic orbital contraction the kinetic energy lowering due to interference [10] (or equivalently "contragradient overlap" [11]) would yield $T < -V/2$. The orbital contraction increases the value of the kinetic energy T (in accordance with the Heisenberg uncertainty principle) by the amount required to reestablish the relation $T = -V/2$. Since this density adjustment must be associated with a *lowering* of the total energy (in accordance with the variation principle), it must be such that the *potential* energy is lowered concomitantly. It is thus apparent that *the atomic orbital contraction necessarily occurs in those regions where the potential energy is lowest.* In H_2 these regions lie near the two nuclei. We shall see that various molecules differ significantly in the location of these regions. (It should be mentioned that, in systems with several valence pairs of different character, the requirement of the virial theorem for the total system is often fulfilled by different types of responses of the different pairs [13].)

From the equilibrium distance (Fig. 1D) on towards shorter distances, the *potential energy* plays an increasingly important role. While, at large and medium distances, each electron experiences on the average one shielded and one unshielded nucleus, at shorter distances each electron experiences both nuclei increasingly as unshielded. At the same time the role of the kinetic energy diminishes because the *interference* between the atomic orbitals *decreases* with *increasing overlap.* (Interference between two 1*s*-type atomic orbitals is maximal when S is about

0.5 and it vanishes for $S=1$ *as well as* for $S=0$; it is approximately proportional to $S(S-1)$ [10].) Consequently, the *density pattern* arising from orbital contraction becomes increasingly dominated by the nuclear attractions. Concomitantly, the repulsion between the nuclei begins to dominate the molecular *energy.*

The preceding discussion shows that, because of the compensating variations due to orbital interference and nuclear shielding, the DD of the H_2 bonding orbital has a *remarkably similar pattern at most internuclear distances*, namely positive values in the central region and negative values in the outlying regions. Only the positions of the nuclei change: at large distances they lie in the negative part of the DD, at medium and short distances they lie in the positive part. *This near constancy of the DD contrasts rather strikingly with the substantive change in the interatomic interaction* from attraction to repulsion, as the atoms approach each other.

Omitted from consideration here are the small density variations at very large distances which accompany van der Waals interactions, and the density rearrangements describing the transition to the united atom at very short distances.

3.2. The non-bonded repulsions between the lone pairs of two helium atoms

Many molecules contain valence electrons which do not participate in bond formation and, in most cases, they occupy lone pair orbitals. It has been recognized since the early days of quantum chemistry that the antisymmetry of many-electron wavefunctions results in the Pauli exclusion effect which, for several doubly occupied orbitals, can be visualized as an apparent repulsion between them. It implies that there exists a tendency for different lone pairs to avoid occupying the same part of space. For example, this tendency is the physical basis for the analysis of molecular geometries by Gillespie and Nyholm [14]. In agreement with this view, an energy increase is observed when two doubly occupied orbitals approach each other. This increase is *kinetic* in character and it is most easily understood if the orbitals are kept mutually orthogonal. (For such a system, this assumption is no loss of generality because of the invariance of a Slater determinant against non-singular orbital transformations.) As the orbitals overlap each other more and more, the orthogonalization requires an increasingly larger insertion of nodes in the orbitals with a concomitant increase in the kinetic energy density ($\hbar^2|\nabla\psi|^2/2m$) in some regions. In agreement with past conventions we shall use the term "non-bonded repulsion" to denote this "quasi-repulsive" effect.

The simplest example is found in the He_2 system. Here, the picture of two electrons occupying the bonding orbital and two electrons occupying the antibonding orbital is equivalent to the picture of two electrons occupying the left-lone-pair orbital and two electrons occupying the right lone-pair orbital. The orbital binding energy of each lone-pair orbital $[-\beta S/(1-S^2)]$ is equal to the average of the orbital binding energy of the bonding orbital $[\beta/(1+S)]$ and that of the antibonding orbital $[-\beta/(1-S)]$. Since the overlap integral S is positive and the resonance integral β is negative, it is apparent that the antibonding orbital is more strongly antibonding than the bonding orbital is bonding, so that the "nonbonding" lone-pair orbitals are in fact somewhat antibonding. There is thus no *qualitative*

difference between antibonding repulsions and non-bonded repulsions; the difference is only one of degree.

The He_2 system yields instructive insights in the behavior of the difference density between two non-bonded lone-pairs. Figs. 1F-K exhibit DD maps of He_2 for various internuclear distances, obtained from MCSCF calculations with large basis sets as discussed in Sect. 2.

At large distances (Fig. 1F, G) the He_2 DD pattern is exactly opposite to the one found in H_2: now electron population is shifted from the central region in the bond into the regions near and around the nuclei. If the He_2 DD is expressed as the sum of a bonding and an antibonding DD, then the bonding DD exhibits the same pattern as that found in H_2, namely accumulation of charge in the center due to constructive interference, whereas the antibonding DD is the result of destructive interference resulting in a displacement of charge from the bond center towards the nuclear region. The latter contribution outweighs the former resulting in a residual charge shift from the bond to the nuclei. This is in complete analogy to the behavior of the orbital energies. Alternatively, the DD can be expressed as the sum of two orthogonal localized orbitals, one left and one right, each of which has a diminished electron density in the bond center and an enhanced density near and "behind" the nuclei due to the mutual orthogonality requirement. In any event, the charge shift implied by the DD patterns shown in Fig. 1F, G is associated with an overall destructive interference of the atomic orbitals which house the lone pairs. This destructive interference causes an increase in the kinetic energy density ($\hbar^2|\nabla\psi|^2/2m$) which is responsible for the antibonding energy, i.e. the nonbonded repulsion. *At large distances* the patterns of the DD's of H_2 and He_2 have therefore the same origin: namely the interference between the localized orbitals on the two atoms, *constructive with kinetic energy lowering in* H_2, *destructive with kinetic energy increase in* He_2.

At shorter distances (Fig. 1H, I) the DD pattern of He_2 changes drastically. In particular the positions of the nodes vary strongly with the internuclear distance. Some charge accumulation remains on the molecular axis "on the outside", at a distance of about $1.5a$ from the center. This feature is most easily understood in terms of the Pauli repulsions. It is similar to the lone pair density patterns found in heavier atoms, even though He has no p-orbitals in its valence shell.

As the nuclei approach each other, the density contracts towards the nuclear and the internuclear region until the negative DD has disappeared between the nuclei (Fig. 1H). *At short distances* (Fig. 1I and K) *the DD pattern becomes somewhat similar to that of* H_2 with a density increase around and between the nuclei. The main difference between H_2 and He_2 is the position of the negative density minima in the outer region. In H_2 they lie on the internuclear axis and vanish in the limit $R \to 0$, where constructive interference disappears. In He_2 the Pauli repulsion causes rather stable local "lone pair" maxima in that region and the main density decrease occurs in an ellipsoidal shell around the molecular center.

At large distances the repulsion between the two helium atoms is essentially caused by the non-bonded repulsion between the two doubly filled atomic lone

pair orbitals and, hence, kinetic in character. At short distances it is however due to the potential repulsion of the two nuclei which become increasingly less shielded from each other by the electron cloud. Thus *the molecular energy curve never changes its repulsive character, even though the DD pattern changes very greatly* - a behavior exactly opposite to that found in H_2!

3.3. Comparison of the results for H_2 and He_2

Our findings on H_2 and He_2 may be summarized as follows. There appears to exist a relation between the energy and the density pattern. However, this relation changes its character with the internuclear distance. To allow a meaningful comparison of the two systems in Fig. 1, those DD maps of H_2 and He_2 are placed next to each other which correspond to similar values of the overlap integral between the two principal atomic orbitals.

At *short distances*, where the overlap is large, say ≥ 0.8, the most prominent effects are due to the unshielded *nuclear coulomb potential*, which causes a density contraction and an overall repulsive interaction. The difference between the interactions in the two molecules manifests itself only in finer details, namely in a quadrupolar charge rearrangement in the outer region which adds or subtracts to the main effect of central contraction.

At *medium distances* with medium overlap values, say $0.2 < S < 0.6$, the driving effect is the change of the *kinetic energy density* resulting from orbital interference. Here bonding interference between the AO's in H_2 results in energy lowering and central charge accumulation, whereas antibonding interference between the AO's in He_2 changes both, energy and density, in the opposite direction.

Finally, at *very large distances* and small overlap, say $S \leq 0.1$, the interaction is of the van der Waals type, Valence-Bond or Spin-Valence type, that is it arises from the *interelectronic interaction* being reduced by correlation effects. In the case of polarizable open d shells in transition metal-atoms, this type of interaction may become quite strong without significantly influencing the density pattern.

In most textbook interpretations of difference density maps, density accumulation between the nuclei is associated with bonding, and density depletion in this region is associated with an antibonding interaction. From the preceding analysis it is obvious that this relation only holds for intermediate overlap values and that the DD pattern is also indicative of the magnitude of the overlap. In H_2 and He_2, with only one interacting orbital per atom, the latter is simply related to the ratio of the internuclear distance to the orbital radius. Considerably more complex DD patterns are to be expected for molecules, which have several orbitals with different overlap strengths for any one internuclear distance, namely core-orbitals, σ type orbitals and π type orbitals. In the following sections we shall examine several such cases.

3.4. Atoms with inner cores

The atomic cores, which exist in all atoms other than H and He, do not participate in the binding process and they are inaccessible to exact X-ray determinations.

Their difference densities are therefore of little interest here [15]. The cores exert however marked effects on the valence shell electrons so that valence shell DD patterns of molecules with cores differ characteristically from those of the core-free molecules H_2 and He_2. First, the Pauli-exclusion pseudo-repulsion prevents the valence electrons from entering the core regions (except for the orthogonalizing tails which establish the filled shell repulsions [15]). As a consequence, the valence electron distributions, second, gain the freedom to assume a wider variety of shapes, a flexibility which is commonly described by the mixing of s, p and possibly d orbitals, and which is related to the near degeneracy of orbitals with different l-quantum numbers.

The pseudopotential approach [16] offers an elegant and effective way of focussing attention on the valence electrons and discussing the just mentioned features without involving the core electrons. For the molecules considered here we require only the effective radial potentials for the 2s and 2p electrons. It turns out that these two are similar for the following reason. The effective potential for an electron in a 2s atomic orbital essentially accounts for the Pauli exclusion repulsion by the $1s$ orbital. The effective potential for an electron in a $2p$ atomic orbital, on the other hand, does not contain such terms, instead it accounts for the centrifugal force arising from the non-vanishing angular momentum which is particularly strong in the core region.

Figure 2 exhibits effective potentials of the cores acting on the valence electrons in several homonuclear diatomic molecules. The potentials of F_2 illustrate the shape of an effective potential for a very electronegative element with a large effective nuclear charge and a small core. Except for very short internuclear distances these potentials are similar to the one of H_2 in that the minima occur near the nuclei and a pronounced maximum exists at the bond center. The potential of Li_2 on the other hand illustrates the shape of an effective potential for an element of low electronegativity with a small effective nuclear charge and an extensive core. Here the potential is flat and comparatively low at the bond center for large and medium distances. For short distances, this potential has a minimum at the bond center which, due to the relatively large cores, is confined to a quite small region.

The shape of the effective potential is expected to have the following effect on the charge distributions. We have explained earlier (Sect. 3.1, p. 475) that the quantum mechanical interference of overlapping AO's accumulates charge in the bond center and that *this charge is drawn from the regions of maximum atomic valence density. These are the regions where the effective potential of the atom has its minima.* Consequently, at larger bond distances (where AO interference is the main effect), DD minima occur for H_2 at the nuclei but, for molecules with cores, they occur at points just outside the cores. At shorter distances the effective potential energy is lowered in the bond region so that charge accumulation in the bond is favored by both, the kinetic and the potential energy. The electron density will therefore increase in the molecular center and the DD minima between the bond center and the atomic cores will be filled in. For electropositive atoms

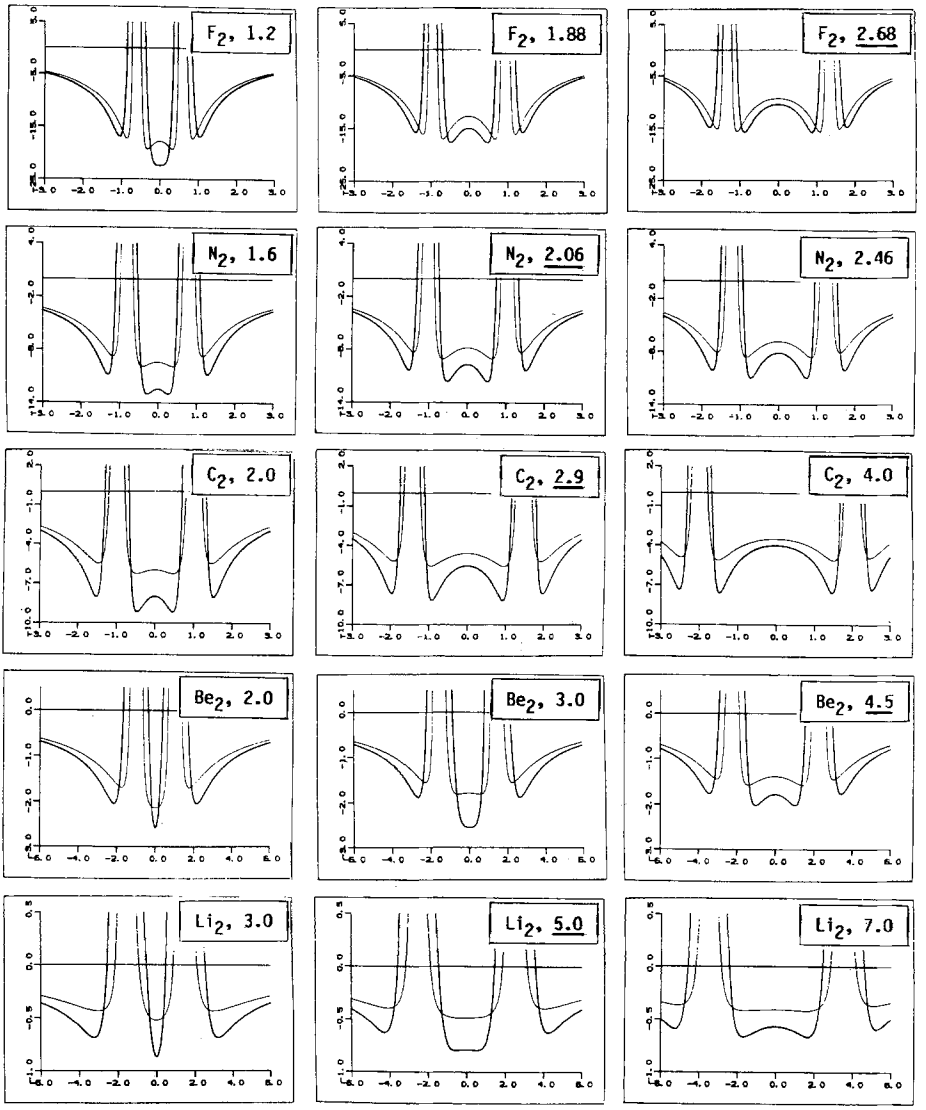

Fig. 2. Effective core potentials for a valence electron in the field of two atomic cores for some homonuclear diatomic molecules, plotted along the molecular axis. *Bold lines:* electrons in s-AOs; *thin lines:* electrons in p-AOs (including the centrifugal potential $l(l+1)/2r^2$). The molecule and the internuclear distance (in bohr) are on each panel. The equilibrium distances are underlined

this occurs already at fairly large internuclear distances, because the potential is low and flat in the bond region. At short distances the large atomic cores have the effect of squeezing the electron density perpendicularly away from the bond axis.

This kind of reasoning, which is based on the pseudo-potential model, will prove useful in *understanding* the DD's to be presented in the subsequent sections. It

should however be noted that, as outlined in Sect. 2, the displayed DD's are in fact *calculated* by all-electron *ab initio* (not pseudo-potential) methods.

3.5. The electron pair bond in Li_2

FORS difference density maps for Li_2 are shown in Figs. 3A–C for the distances 7 bohr, 5 bohr (approximately the equilibrium distance) and 3 bohr, respectively.

At large distances the DD is similar to that found in H_2 at large distances (Fig. 1A). Still there are three characteristic differences. First, because of the diffuse nature of the Li valence shell only small DD values occur. Second, while the *integrated* population change in the core regions is insignificant, there occur local

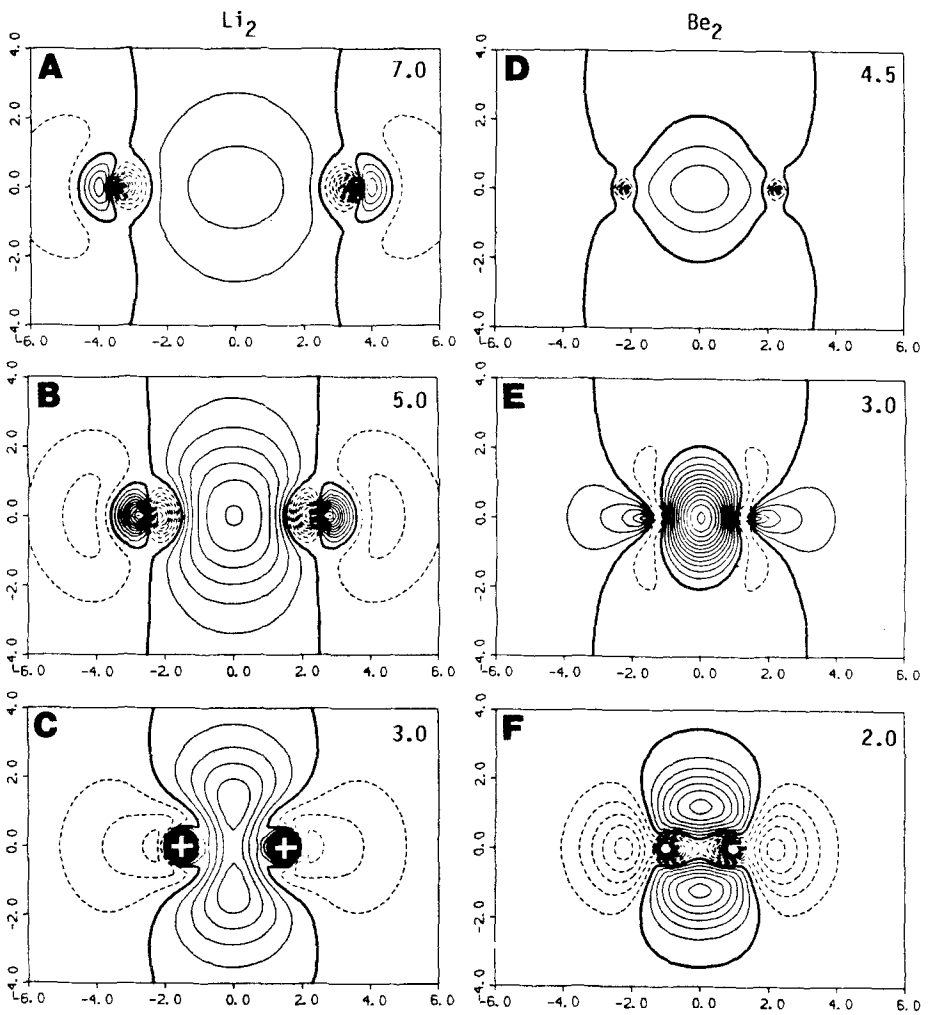

Fig. 3A–F. Difference densities for Li_2 and Be_2. The internuclear distance (in bohr) is indicated on each panel. Increments between adjacent contours for Li_2 are 0.001 e/a^3. The increments for Be_2 are 0.04 e/a^3, i.e. identical to those indicated in the last paragraph of Sect. 2

charge shifts as depicted by the dipolar DD distribution near the nuclei. They are due to the orthogonalization of the valence tails from the other atom and are related to the nonbonded repulsion between the inner shell and the bonding orbitals [15]. Finally, because the effective valence potential in Li_2 is flat between the nuclei (Fig. 2), the accumulation of charge in the bond due to interference is further increased by charge contraction towards the center of the bond, whereas in H_2 the charge contraction, when it occurs, is directed towards the nuclei.

Furthermore, whereas in H_2 the region of density increase remains about equal in size when the internuclear distance decreases, in Li_2 this region is becoming constricted by the intrusion of the extended cores (see Fig. 3C). At $R = 3$ bohr the density maxima lie on a torus around the bond center. Moreover, because of the large overlap (0.79 at this distance) the cores are less shielded. They are therefore embedded in a significantly contracted charge cloud which results in a density increase of about 0.31 e/Å^3 inside the core.

3.6. The non-bonded repulsions in Be_2

FORS difference density maps for Be_2 are presented in Fig. 3D–F. For $R > 4a$ the molecular energy curve of Be_2 is nearly constant. It has an extremely shallow minimum between 4.5 and $5a$ [17].

The existence of the Be core results in the near-degeneracy between the 2s and 2p orbitals, as mentioned earlier, and this leads to two flexibilities: orbital polarization and non-dynamical electron correlation. Both effects counteract the non-bonded repulsions between the occupied 2s shells in Be_2 so that the DD's of Be_2 and He_2 are markedly different.

The effective potential in Be_2 is flat around the bond center (except for very short internuclear distances), similar to the one in Li_2 (Fig. 2). As in Li_2, there occurs therefore a charge accumulation in the "bond" of Be_2 (Figs. 3A, B and 3D, E) even though the interatomic interaction is very small for the larger distance (Fig. 3D) and quite repulsive for the shorter distance (Fig. 3E). These observations suggest that charge accumulation between atoms may have a good deal to do with the shape of the effective potential regardless of the binding or antibinding interaction.

The Be_2 and He_2 DD maps have one feature in common, namely the "lone-pair-type" charge accumulations at the ends of the molecules (Figs. 1I and 3E). They are undoubtedly a result of the nonbonded repulsions of the overlapping s shells. By contrast, there occurs a charge depletion in these regions for the Li_2 molecule which has only one valence pair.

As a curiosity we finally show the difference density of Be_2 for $R = 2a$ (Fig. 3F). At this short distance the Pauli repulsion between the atomic 2s-shells is so large that it squeezes the valence electrons from the 2s, 2pσ-NOs into the 2pπ-NOs through a strong configuration interaction between $2\sigma_g^2 2\sigma_u^2$ and $2\sigma_g^2 2\pi_u^2$. (A similar configuration interaction is ineffectual in He_2 because, in the absence of inner cores, the effective potentials for s and p electrons are very different.) The

configuration interaction completely reverses the sign of the DD-maps in Be_2 as compared with those of He_2 (Fig. 1H), even though the interatomic interaction is repulsive in both cases. Fig. 3F illustrates that there are cases where configuration interaction does influence the one-electron density significantly. A similar squeezing of the valence electrons by the approaching cores was also observed in Li_2 (Fig. 3C), whose effective potential has a similar shape as that of Be_2 (Fig. 2).

4. Analysis of the difference density in F_2

There are several reasons why an analysis of the DD of F_2 is attractive. The molecule contains σ and π electrons and also several lone pairs. Yet the bond is simple. Moreover, the atom has a degenerate ground-state which raises important questions regarding the appropriate definition of the difference density.

4.1. Total difference density at the equilibrium distance

The total electron difference density for the F_2 molecule at the equilibrium internuclear distance $R_e = 2.68a$ is shown in Fig. 4. From the FORS density of F_2 the densities of two ground state atoms are subtracted. They are assumed to be in the ^2P_z state with the singly occupied $2p\sigma$-AOs pointing towards the other atom and thus overlapping to form the bond. This definition of the density difference of F_2 was first proposed by Bader et al. [18].

Figure 4A shows a slight density decrease at larger distances all around the molecule, indicating an *overall orbital contraction* upon bond formation. The *density increase* of 0.37 e/Å^3 *at the molecular center*, although somewhat small in comparison with other σ-bonds between second row atoms (for instance between C atoms [2–5] with DD's of about 0.6 e/Å^3), seems reasonable for a weak σ-bond. There are *pronounced density depressions* (-0.79 e/Å^3) *on the internuclear axis* between the bond center and the occupied atomic cores. The *density increase of* 0.44 e/Å^3 behind the cores is typical for *lone pair regions*, although again somewhat low. (Compare, e.g. the results for N_2, shown in Sect. 5.)

4.2. Effects of correlation and basis set extension

Before examining the detailed features in Fig. 4A we consider the correlation and basis-set effects. The density difference at the SCF level is very similar to the one found by Bader et al. [18] and is shown in Fig. 4B; the *correlation density*, i.e. the difference between Fig. 4A and B, is shown in Fig. 4C. Although the FORS method includes only "internal" correlations and thus omits certain "semi internal" correlations, which contribute markedly to the binding energy of F_2 [19], our correlation density is very similar to the one obtained by Schweig et al. [2] with an SCF-CI approach. It is seen that correlation enhances the long-range density contraction and the density increase in the lone pair region. It furthermore attenuates the SCF density changes between the atoms: the central SCF maximum of 0.51 e/A^3 is reduced to the aforementioned low value of 0.37 e/A^3, and the extremely strong SCF depressions of -1.45 e/A^3 are about

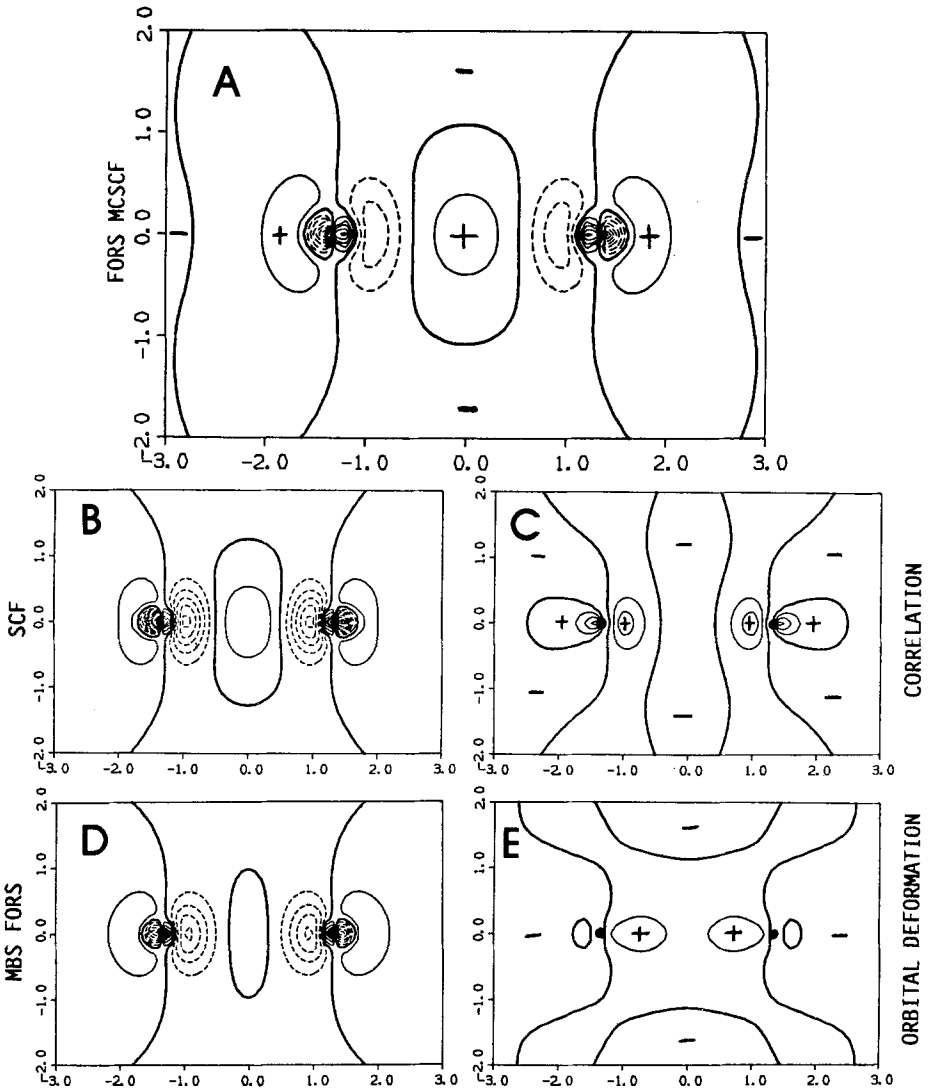

Fig. 4A–E. Difference densities for F_2 at $R_e = 2.68a$ for various approximations to the exact electronic wavefunction. Panel **C**: difference between **A** and **B** = correlation contribution. Panel **E**: difference between **A** and **D** = contribution from basis set extension, i.e. orbital deformation. Contour values as indicated in Sect. 2, last paragraph

half filled in. This large correlation correction is well above the limit of detectability and much larger than correlation effects that are usually met in valence shells [20].

The density difference of Fig. 4D is calculated from a FORS function obtained with unmodified *atomic* SCF orbitals. The difference between Figs. 4A and 4D therefore represents the molecular density deformation due to orbital contraction and polarization. It is shown in Fig. 4E. This *orbital deformation* has a similar

effect as correlation in as much as it contributes to both the overall density contraction and to the filling-in of the unusual density depressions between the atoms. However it counteracts correlation by increasing the central maximum by $0.17\ e/A^3$.

4.3. Decomposition in terms of FORS natural orbital contributions

From the expansion coefficients the principal atomic contributors to the FORS NO's are readily recognized to be as follows:

The NO's $1\sigma_g$, $1\sigma_u$, both of which have an occupation number of 2, are mainly composed of the 1s AO's.

The NO's $2\sigma_g$, $2\sigma_u$, both of which have occupation numbers very close to 2, are mainly composed of the 2s AO's.

The NO's $3\sigma_g$ (occupation number = 1.868) and $3\sigma_u$ (occupation number 0.137) are mainly composed of the $2p\sigma$ AO's.

The NO's $1\pi_u$ (occupation number = 4) and $1\pi_g$ (occupation number = 3.997) are mainly composed of the $2p\pi$ AO's.

Consequently it is meaningful to form the difference densities between the FORS NO's and the corresponding free atom AO's.

The total FORS difference density of Fig. 4A is reproduced in Fig. 5A. It is decomposed into the three additive contributions of Fig. 5B–D.

Figure 5B embodies the difference density which is the sum of the contributions from the orbitals $1\sigma_g$, $1\sigma_u$, $2\sigma_g$, $2\sigma_u$ as explained above. Since all of these orbitals are doubly occupied, the density difference reflects the *non-bonded repulsions*, acting on the occupied atomic 1s and 2s orbitals, which can be associated with the Pauli exclusion principle. It leads to a polarization of the 1s shell [15] and the 2s shell and is responsible for the observed density depletion between the nuclei and the corresponding density increase behind the nuclei in the lone pair region.

Figure 5C embodies the density difference

$$[1.868(3\sigma_g)^2 + 0.137(3\sigma_u)^2] - 1.0025[(2p\sigma_{\text{left}})^2 + (2p\sigma_{\text{right}})^2],$$

which is associated with the formation of the bond. It is manifestly responsible for the density accumulation in the bond center. It shows the typical behavior of covalent interactions at relatively large internuclear separations: a density increase in the bond center and a slight density decrease in the outer region and in the vicinity of the nuclei, i.e. density changes due to orbital interference which are associated with a kinetic energy decrease and a slight potential energy increase. There is one characteristic difference between H_2 and F_2 in that, in the latter, the immediate vicinity of the nuclei belongs to the 1s inner shells from which the valence electrons are excluded as discussed in Sect. 3.4. Therefore, instead of a density decrease *at the nuclei*, as observed in H_2 at larger distances, one finds in

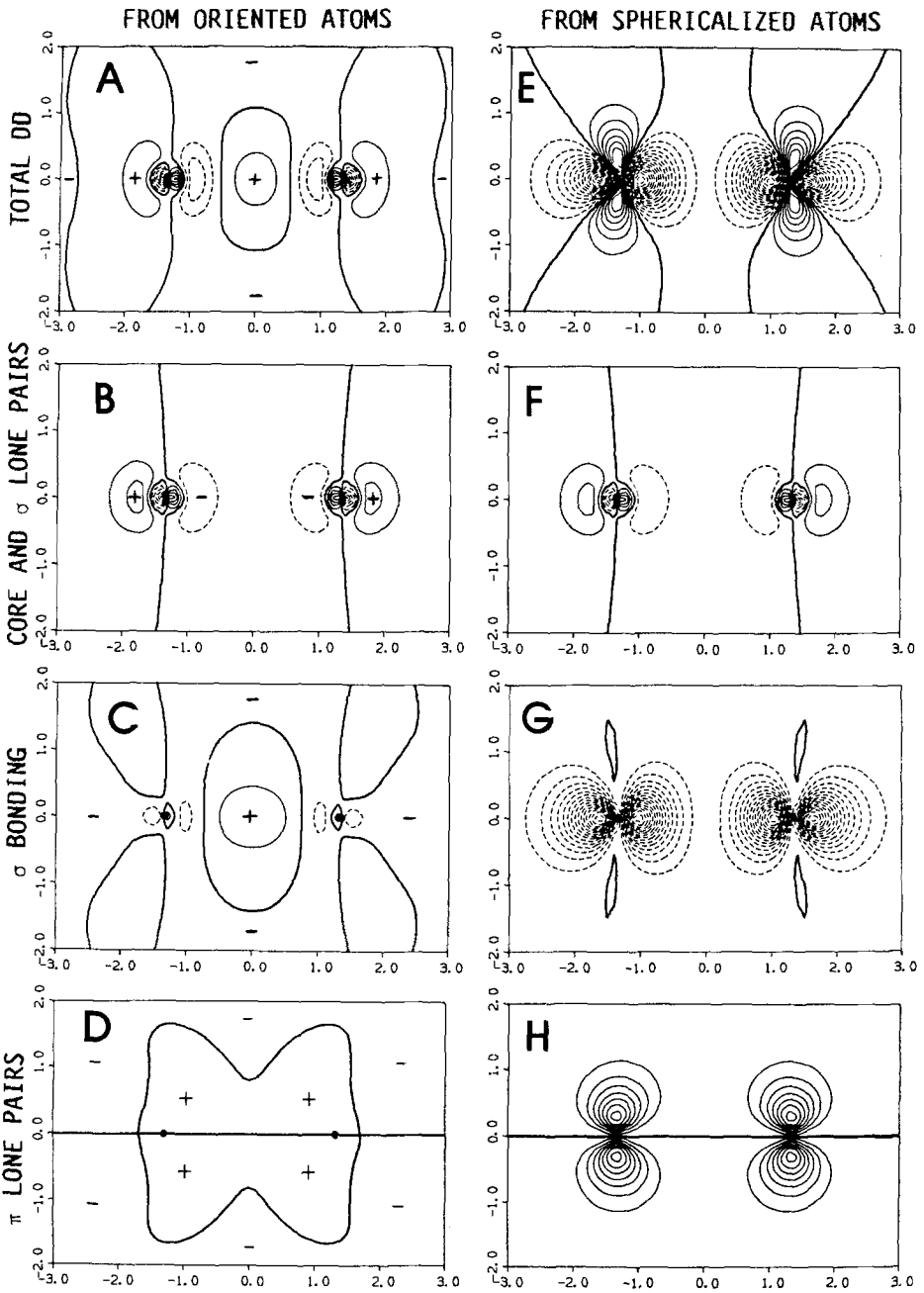

Fig. 5. Natural orbital contributions to FORS difference densities of F_2 at $R_e = 2.68a$. Panels **A–D**: atomic reference density = sum of two oriented F atoms in ^2P_z states. Panels **E–H**: atomic reference density = sum of two spherically averaged F atoms obtained from the ^2P_x, ^2P_y, ^2P_z states. Panels **A** and **E**: total DD. Panels **B** and **F**: eight-electron contributions from ($1\sigma_{g,u}$, $2\sigma_{g,u}$-NOs minus 1s, 2s-AOs). Panels **C** and **G**: two electron contribution from ($3\sigma_{g,u}$-NOs minus $2p_z$-AOs). Panels **D** and **H**: eight-electron contributions from ($\pi_{g,u}$-NOs minus $2p_{x,y}$-AOs). Contour values as stated in Sect. 2, last paragraph

F_2 a density decrease in the "*inner parts*" *of the valence region* "right outside the 1s cores".

Figure 5D shows the difference between the nearly completely filled NO's $1\pi_u$, $1\pi_g$ and the sum of the π-AO densities. This density difference is very small everywhere (<0.1 e/Å^3), implying a small interaction between the $2p\pi$ AO's, a fact which is related to the comparatively large equilibrium distance.

In summary, the difference density decomposition in terms of FORS NO contributions permits characteristic details of the total density difference to be associated with specific interactions, namely the Pauli repulsion between the non-bonded *s* AO's and the covalent interference between the half filled $2p\sigma$ AO's.

4.4. Spherically averaged versus oriented atomic reference densities

It is a commonly accepted practice to define experimental or theoretical density differences by subtracting the atoms in their neutral ground states from the molecule. In the case of degenerate ground states, most authors subtract the *spherically averaged* atomic density since it is the simplest unique choice [2–5]. In the case of fluorine this is $(2p\pi^{10/3}2p\sigma^{5/3})^2\bar{P}$. The density difference obtained with this definition is presented in Fig. 5E. It exhibits a quadrupolar pattern with enormous maxima in the atomic $2p\pi$-AO region and corresponding minima on the molecular axis on both sides of the nuclei (DD < -5 e/Å^3). It exhibits *no* density increase anywhere on the bond path nor in the lone pair region [32].

The breakdown into NO-contributions, given in Figs. 5F–H, demonstrates that this density difference is dominated by the transfer of 4/3 electrons from the atomic $2p\sigma$ to the $2p\pi$ AOs, which essentially reestablishes the oriented free atoms in the form they were used in the preceding section. This apparent density transfer, which has caused some discussion in the past [21], therefore simply reverses the averaging process by which the artificial atomic reference densities were formed. It is typical for bonded atoms with degenerate groundstates, such as B, C, O and F when located in sites of low local symmetry, and it is an order of magnitude larger than the DD-values obtained with oriented F atoms as is evident from the left side of Fig. 5. It completely swamps the fine details which are significant for the formation of the bond and which were discussed and explained in the preceding section.

In order to confirm this interpretation we formed, for a *free* F *atom*, the difference between the oriented ^2P_z groundstate density and the spherically averaged groundstate $^2\bar{P}$ density. We then superimposed these two *purely atomic* differences for two atoms placed at a distance 2.68 bohr from each other. The resulting difference map is shown in Fig. 6B. Manifestly, it is extremely similar to the density in Fig. 6A, which is the same as that of Fig. 5E, i.e. the *molecular* difference formed with spherically averaged atoms. The latter therefore demonstrates that atoms which, in their free states, have quadrupolar density distributions, do maintain these distributions in an oriented manner, when they are embedded in certain molecules. In such cases, *spherically averaged atoms form suitable promolecules*

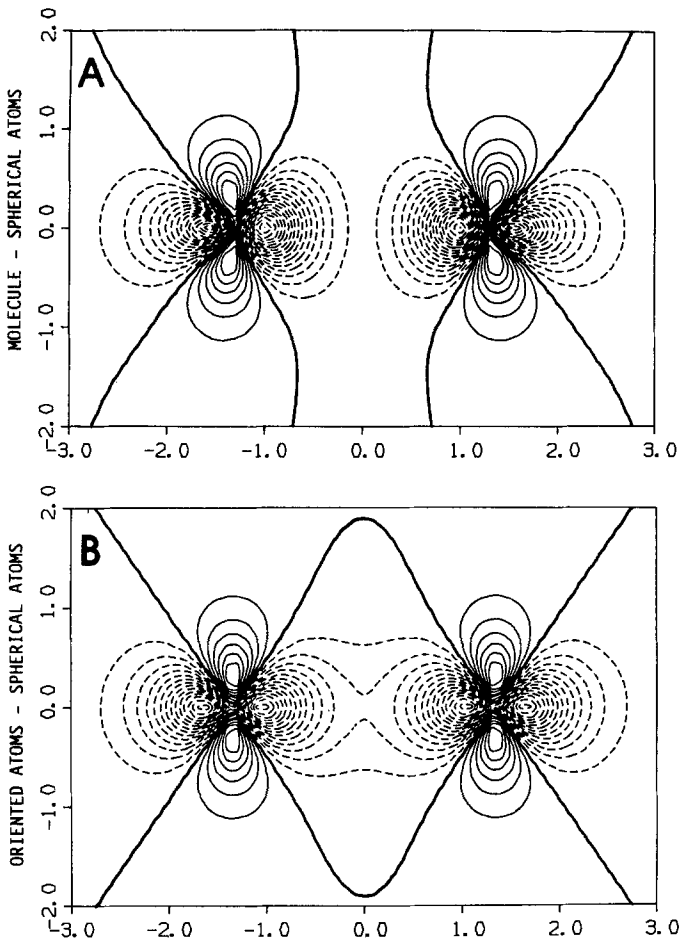

Fig. 6A, B. Comparison of atomic and molecular FORS difference densities at $R_e = 2.68a$. Panel **A**: molecular density of F_2 minus sum of densities of spherically averaged F atoms. Panel **B**: sum of densities of two oriented F atoms in ^2P_z states minus sum of densities of two spherically averaged F atoms. Contour values as stated in Sect. 2, last paragraph

for exhibiting orientations of atoms in molecules, but they provide inappropriate promolecules for identifying density features that characterize binding effects, which are an order of magnitude smaller.

The appropriate choice of the atomic reference density is trivially obvious in F_2. It is the ^2P_z density with the populations $(2p\pi^4 2p\sigma^1)$. A general definition and a method for determining unique and useful atomic reference densities at sites of low symmetry in any specific molecule will be given elsewhere [22]. It leads to ^2P_z in the case of F_2.

We shall denote a density difference as a *Chemical Difference Density* (CDD) if it is constructed with appropriately oriented atomic reference states.

4.5. Dependence of the difference density upon the internuclear distance

The F_2 bond is unusually *long*. For example, scaling a typical C—C single bond length of $2.9a$ by the ratio of the effective nuclear charges of C ($Z = 3.3$) and F ($Z = 5.3$), one would expect a F—F bond length of about $1.8a$. In fact, the experimental value is nearly one and a half times as large. It is generally accepted [23] that this unusual bond length is due to the non-bonded repulsions (Pauli repulsions) between the large number of lone pairs.

It is therefore of interest to examine the difference densities for bond lengths shorter than $2.68a$. Figs. 7A–D exhibit the total difference densities of F_2 for the internuclear distances $R = 2.68a = R_e$, $0.9R_e$, $0.8R_e$ and $0.7R_e = 1.88a \approx$ the scaled CC bond length. It is seen that, by the time R is reduced to the latter value, the difference density map exhibits "normal" features, i.e. strong maxima in the bond center and no density depressions between the two nuclei.

Fig. 8 furnishes the breakdown of the total difference density at $R = 1.88a$. Fig. 8B shows that, at the shorter distance, with the stronger non-bonded Pauli repulsions, the density depletion between the atoms and the corresponding density increase in the lone pair regions behind the atoms are considerably stronger. Fig. 8C shows that, at the shorter distance, the $2p\sigma$-overlap is more favorable and causes a much stronger density accumulation between the atoms. In fact, it is so substantial that it greatly overcompensates the density reduction shown in Fig. 8B between the nuclei. Fig. 8D shows that, at the shorter distance, even the $2p\pi$ interactions are strong enough to cause some density changes in the π-system.

Figs. 8E–H show the corresponding density differences which result when spherically averaged atoms are chosen as pro-molecular reference states. These maps demonstrate again that the purely atomic orientation effects, substantiated by Fig. 6, still swamp the chemically significant density differences of Figs. 8A–D, even though the latter are much stronger at the shorter ("normal") distance.

4.6. Canonical SCF-MO versus FORS-NO contributions

The comparison of Figs. 4A and B showed that, at the equilibrium distance $R_e = 2.68$ bohr, the total SCF density difference is qualitatively similar to the total FORS density, and this was also found to be so for the π-contributions. The same similarity exists at the distance $R = 1.88$ bohr (the maps are not shown).

The situation is different for the σ contributions, which are shown in Fig. 9 for $R_e = 2.68$ bohr and in Fig. 10 for $R = 1.88$ bohr. We have seen that, in the FORS approach, the formation of natural orbitals yields NO's with high occupations and NO's with low occupations. The former are $2\sigma_g$, $2\sigma_u$ (occupations close to 2) which have lone pair character with non-bonded repulsions (density depletion between the nuclei, density increase on the outside). The latter are $3\sigma_g$ and $3\sigma_u$ (occupations 1.868 and 0.137 respectively at R_e) and they establish the bond (density accumulation in the bond center). This clean separation into σ lone-pair NO's and σ-bonding NO's corresponds to the concept of chemically active frontier orbitals.

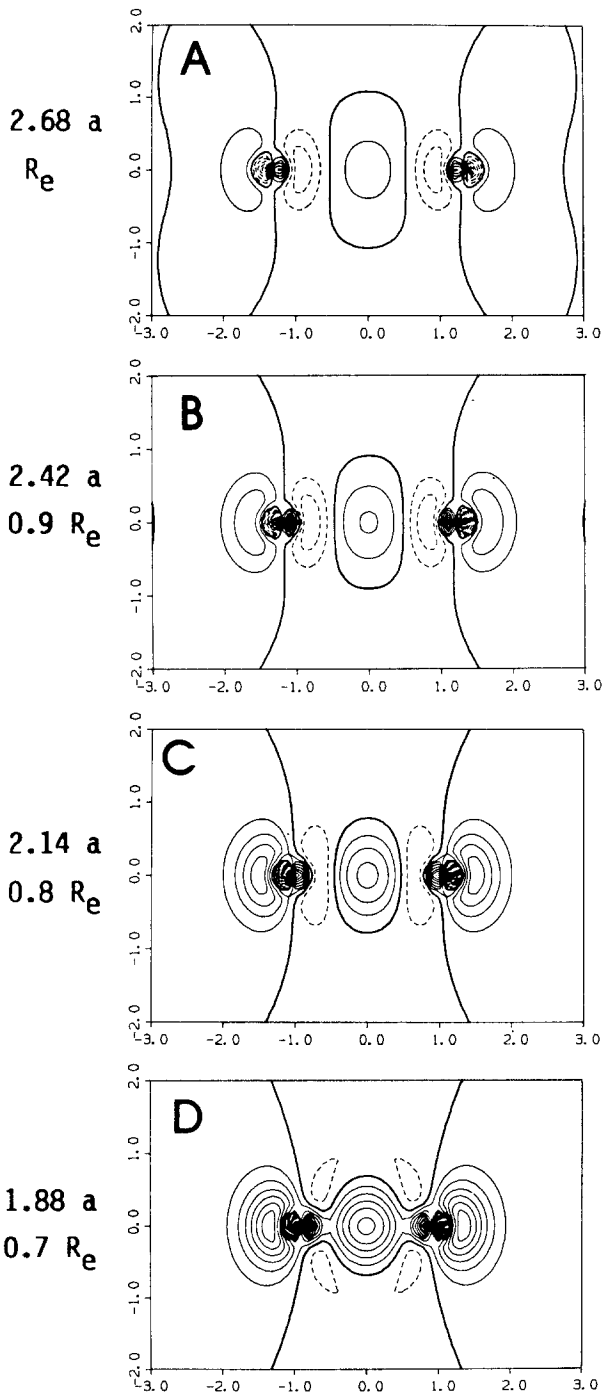

Fig. 7A–D. Total FORS difference densities of F_2 for different internuclear distances, as indicated next to each panel. Contour values as stated in Sect. 2, last paragraph

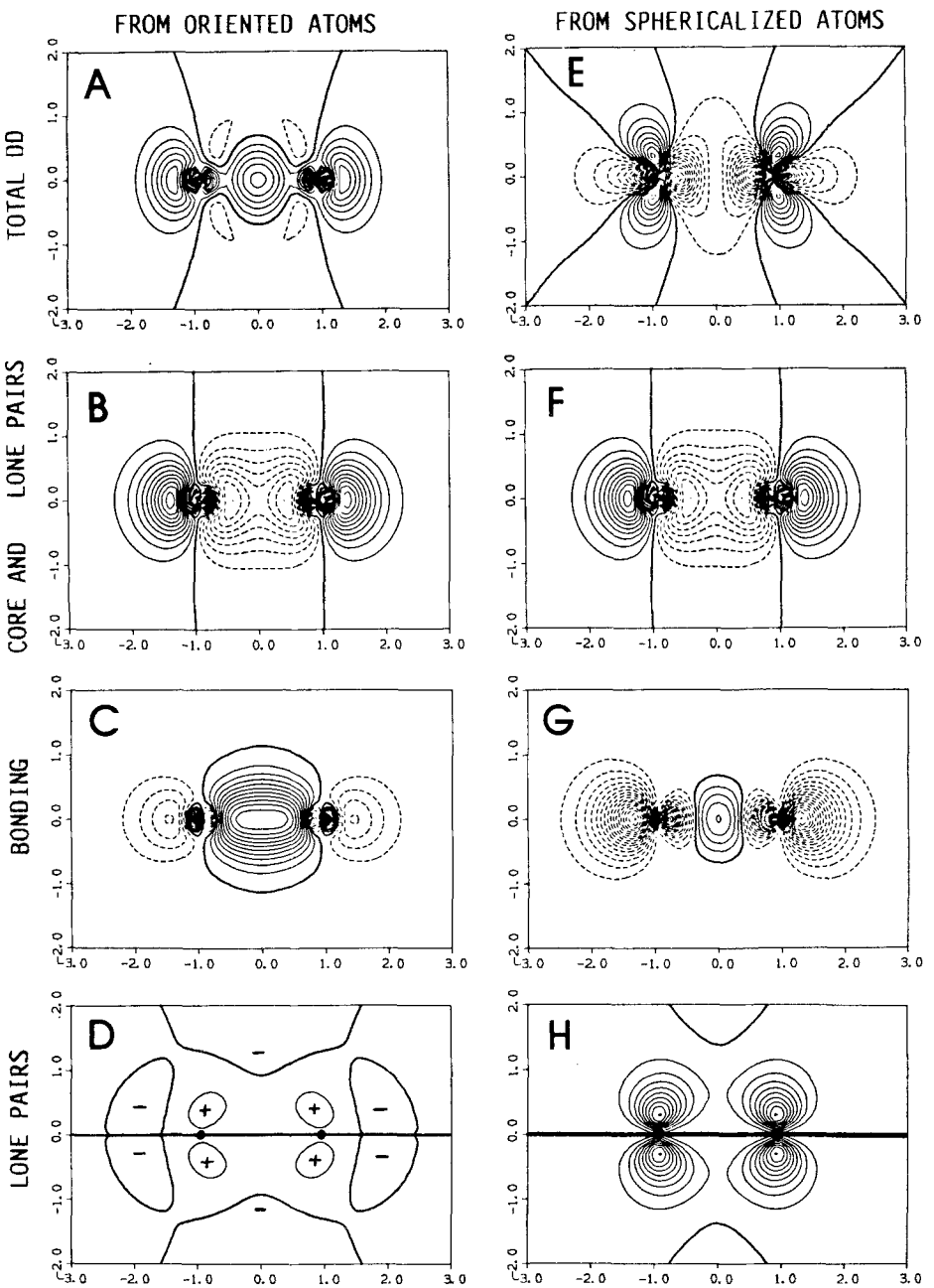

Fig. 8A–H. Natural orbital contributions to the FORS difference density in F_2 at $R = 1.88a$. (≈normal length of an unstretched covalent σ-bond). Panels **A–D**: atomic reference density = sum of two oriented F atoms in ^2P_z states. Panels **E–H**: atomic reference density = sum of two spherically averaged F atoms obtained from the ^2P_x, ^2P_y, ^2P_z states. Panels **A** and **E**: total DD. Panels **B** and **F**: eight-electron contributions ($1\sigma_{g,u}$, $2\sigma_{g,u}$-NOs minus 1s, 2s-AOs). Panels **C** and **G**: two electron contributions ($3s_{g,u}$-NOs minus $2p_z$-AOs). Panels **D** and **H**: eight-electron contributions ($\pi_{g,u}$-NOs minus $2p_{x,y}$-AOs). Contour values as stated in Sect. 2, last paragraph

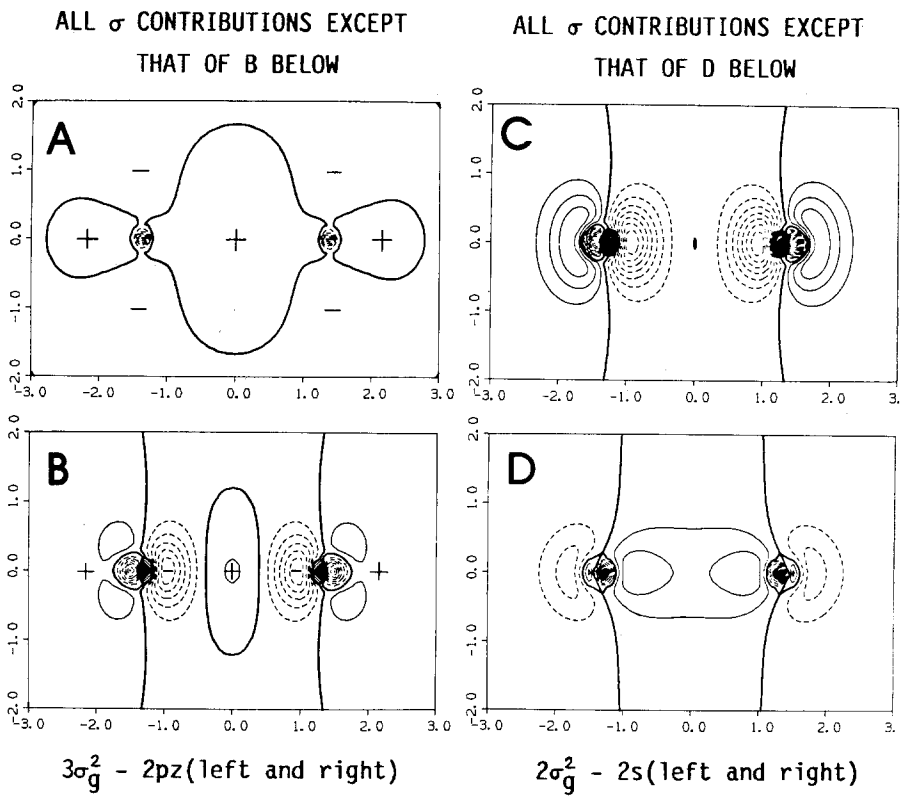

Fig. 9A–D. Canonical MO decompositions of the σ contribution to the SCF difference density of F_2 at $R_e = 2.68a$. Panel **A**: eight-electron contribution ($1\sigma_{g,u}$, $2\sigma_{g,u}$-MOs minus $1s$, $2s$-AOs). Panel **B**: two-electron contribution ($3\sigma_g$-MO minus $2p_z$-AOs). Panel **C**: eight-electron contribution ($1\sigma_{g,u}$, $2\sigma_u$, $3\sigma_g$-MOs minus $1s$, $2s$, $2p_z$-AOs). Panel **D**: two-electron contribution ($2\sigma_g$-MO minus $2s$-AOs). Contour values as stated in Sect. 2, last paragraph

By contrast, the canonical SCF MO's do not furnish such a clean separation. Here, both the $2\sigma_g$ and $3\sigma_g$ MO's have strong admixtures from the atomic $2s$ and $2p\sigma$ AO's. This is so because of the variational character of the Fock equation: it selects orbitals with high and low orbital energies (not occupation numbers!) for a given total electron density. Because of this ambiguity we consider two alternative ways of forming density differences:

First choice:

$(1\sigma_g^2+1\sigma_u^2+2\sigma_g^2+2\sigma_u^2)-(1s^2, 2s^2$ on both atoms): Figs. 9A, 10A;

$(3\sigma_g^2)-(2pz^1$ on both atoms): Figs. 9B, 10B;

Second choice:

$(1\sigma_g^2+1\sigma_u^2+3\sigma_g^2+2\sigma_u^2)-(1s^2 2s^1 2pz^1$ on both atoms): Figs. 9C, 10C;

$(2\sigma_g^2)-(2s^1$ on both atoms): Figs. 9D, 10D.

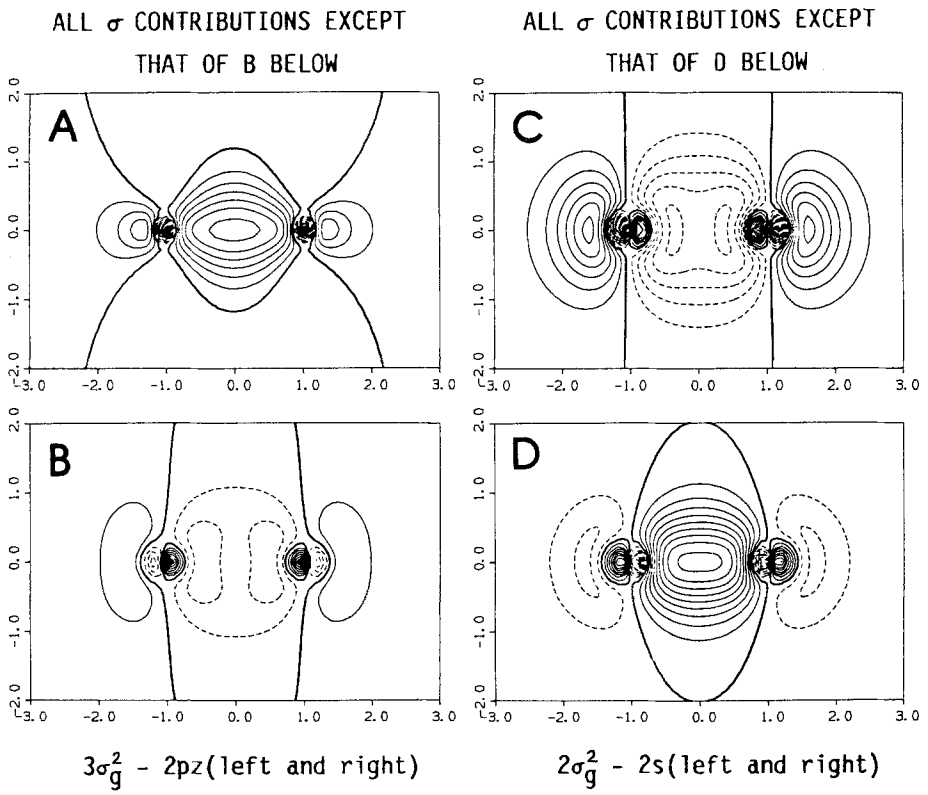

Fig. 10A–D. Canonical MO decompositions of the σ contribution to the SCF difference density of F_2 at $R = 1.88a$. Panel **A**: eight-electron contribution ($1\sigma_{g,u}$, $2\sigma_{g,u}$-MOs minus 1s, 2s-AOs). Panel **B**: two-electron contribution ($3\sigma_g$-MO minus $2p_z$-AOs). Panel **C**: eight-electron contribution ($1\sigma_{g,u}$, $2\sigma_u$, $3\sigma_g$-MOs minus 1s, 2s, $2p_z$-AOs). Panel **D**: two-electron contribution ($2\sigma_g$-MO minus 2s-AOs)

It is apparent that the lone pair characteristics go more with the $3\sigma_g$ MO and that bonding goes more with the $2\sigma_g$ MO's. Although the second choice is somewhat more satisfactory, neither of the two options yields a really satisfactory decomposition of the total density into individual contributions with simple physical meanings. Both suffer from exaggerated cancellations between large positive and negative contributions to the DD, especially at shorter distances.

5. Analysis of the difference density in N_2

We want to confirm the method of interpretation which we used for the F_2 bond by using it also for the very different N_2 bond. The groundstate of the N atom has ^4S symmetry. Its density is spherically symmetric and the problem of orienting the reference density does not arise in the formation of the DD.

The total FORS difference density at the equilibrium distance of $R_e = 2.06a$ is exhibited in Fig. 11A. It is very similar to the SCF-CI-DD map of Schweig et al. [2]. Figure 11B–D shows the FORS-NO contributions, similar to those presented

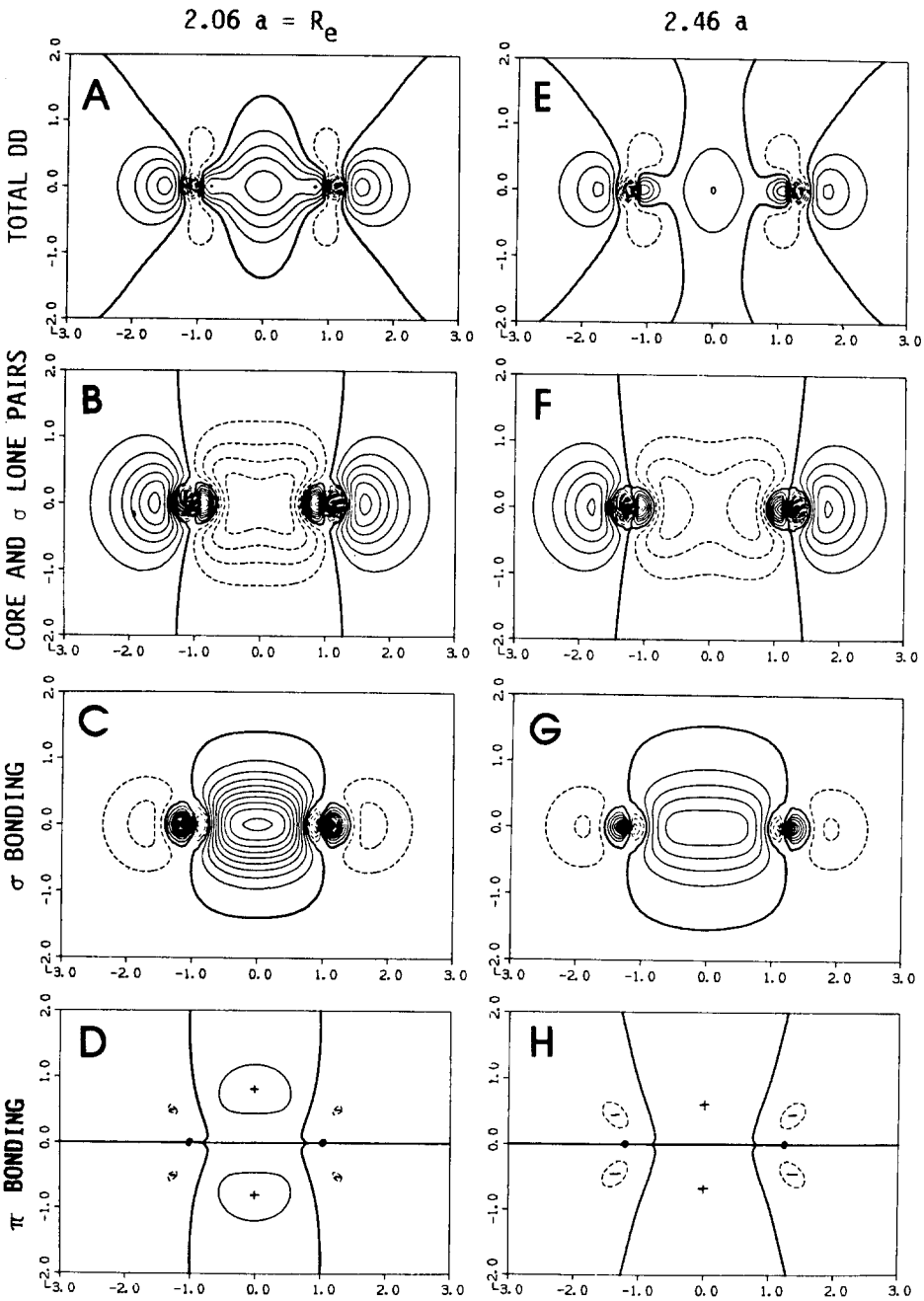

Fig. 11A–H. Natural orbital contributions to the FORS difference density in N_2 at two internuclear distances. Panels **A–D**: $R = R_e = 2.06a$. Panels **E–H**: $R = 2.46a$ (≈normal length of an uncompressed single σ-bond). Panel **A** and **E**: total DD. Panels **B** and **F**: eight-electron contribution ($1\sigma_{g,u}$, $2\sigma_{g,u}$-NOs minus 1s,2s-AOs). Panels **C** and **G**: two-electron contribution ($3\sigma_{g,u}$-NOs minus $2p_z$-AOs). Panels **D** and **H**: four-electron contribution ($\pi_{g,u}$-NOs minus $2p_{x,y}$-AOs). Contour values as stated in Sect. 2, last paragraph

in Fig. 5B–D for F_2. Because of the π-bonds the σ-system in N_2 is *compressed*, which is opposite to the situation in F_2. A "normal" single σ-bond length for an effective nuclear charge of $Z = 3.9$ would be expected to have a length of about $R = 2.46a$. Difference densities for this length are shown in Figs. 11E–H.

The contributions of the core and lone-pair σ-electrons to the DD are shown in Fig. 11B, F. They are qualitatively very similar to the nonbonding contribution in F_2 (Figs. 5B and 8B) and, also, to the total DD of He_2 at medium large distances (Fig. 2G). One might wonder why these nonbonded DD's are qualitatively different from the total DD of Be_2 (Figs. 3D, E) which also has a nonbonded $1\sigma_{g,u}^4 2\sigma_{g,u}^4$ configuration. The reason is that, in Be_2, the nonbonding $2\sigma_{g,u}$ orbital pair can freely mix in 2p AO's which are not needed for any other purpose. In N_2 and F_2 these 2p-AO's are occupied by other valence electrons and, in He_2, the p-AO's are lying at too high energies for effective mixing.

The contribution of the σ-bonding pair ($3\sigma_g^{1.98} 3\sigma_u^{0.02}$) in N_2 (Fig. 11C, G) is also similar to that found in F_2 at the "normal" bondlength (Fig. 8C). The *bonding*

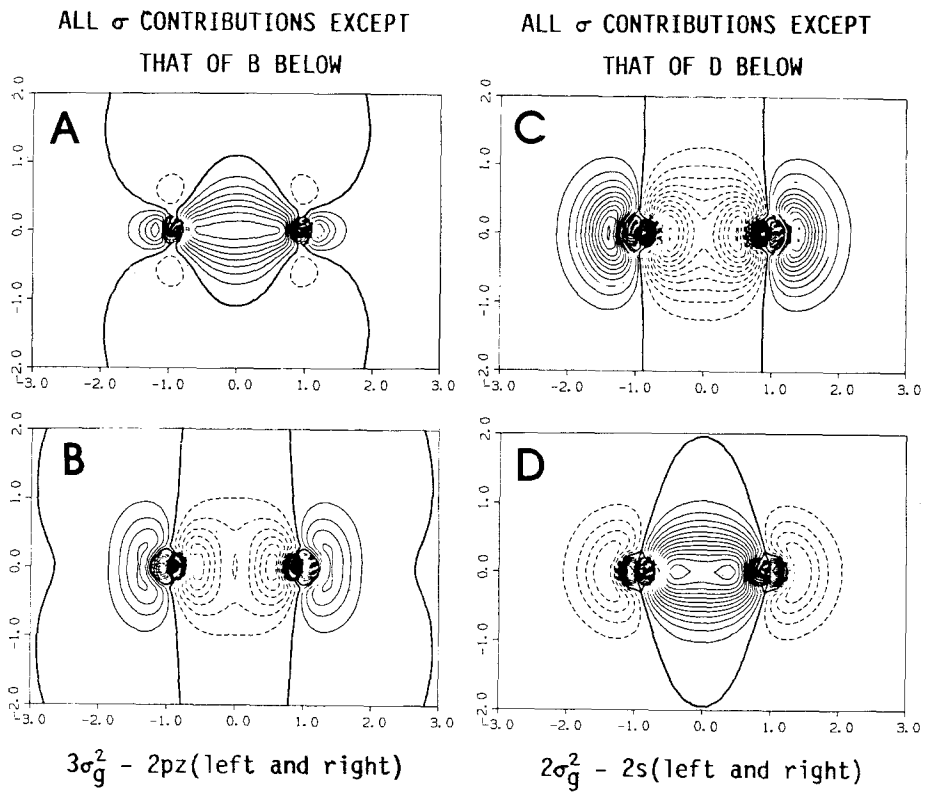

Fig. 12A–D. Canonical MO decompositions of the σ-contribution to the SCF difference density of N_2 at $R_e = 2.06a$. Panel **A**: eight-electron contribution ($1\sigma_{g,u}$, $2\sigma_{g,u}$-MOs minus 1s,2s-AOs). Panel **B**: two-electron contribution ($3\sigma_g$-MO minus $2p_z$-AOs). Panel **C**: eight-electron contribution ($1\sigma_{g,u}$, $2\sigma_u$, $3\sigma_g$-MOs minus 1s, 2s, $2p_z$-AOs). Panel **D**: two-electron contribution ($2\sigma_g$-MO minus 2s-AOs). Contour values stated in Sect. 2, last paragraph

π-contribution of $(\pi_u^{3.87}\pi_g^{0.13})$ in N_2 (Fig. 11D, H) differs of course from the *nonbonding* π-contribution in F_2 (Fig. 8D). Although the π-interaction in N_2 is small, even at R_e, it is typical covalent in character: charge is transferred from the inner valence shell region to the overlap region. Because of the beginning π-orbital contraction, the density depression near the atomic cores is smaller at R_e than at $R = 2.46a$.

As was the case for F_2, canonical SCF orbitals are found to be less suitable for a decomposition of the DD of N_2 into physically meaningful contributions. Figure 12A shows the $1\sigma_{g,u}2\sigma_{g,u}$ contribution, Fig. 12B shows the $3\sigma_g$ contribution. As in F_2 (Figs. 9D, 10D), the most strongly bonding orbital is the lowest valence orbital (Fig. 12D), whereas the higher MO's $2\sigma_u$, $3\sigma_g$ (Fig. 12C) have the character of two lone pairs.

In N_2 the difference density is positive everywhere on the axis between the two nuclei, except in the small inner shell core region. This is so for R_e as well as for distances up to the "normal single bond length" of $R = 2.46a$ (Fig. 11A and E). It also holds true for H_2 at R_e (Fig. 1D) and for F_2 at the "normal single bond length" of $R = 1.88a$ (Fig. 7D). At *larger* internuclear distances two negative difference density minima occur *on* the axis between the two atoms in N_2 as they do in F_2 (Fig. 7A-C) and in H_2 (Fig. 1A, B). This is so because, at these distances, AO interference shifts density from the inner valence shell (i.e. the region of low effective potential, see Fig. 2) to the bond center, while orbital contraction towards the effective potential minima does not yet occur. It *suggests that two such regions of density depletion are indicative of an expanded or abnormally long bond.*

6. Conclusions and inferences

6.1. Fundamental problems

The study of electron densities is motivated by the hope of being able to identify features that will elucidate the nature of chemical bonding under various conditions. Not only do electron densities have an immediate conceptual appeal, but there moreover exist two theorems which relate them to dynamical quantities. The Hohenberg-Kohn Theorem [24] asserts that the total density contains the same information as the N-electron wavefunction and that there exists a functional which yields the energy in terms of the density. The Hellmann-Feynman Theorem [25] on the other hand provides a simple formula for calculating the forces between the atoms in a molecule from the exact electron density.

Why then has it proven to be so difficult to relate questions of chemical bonding to electron densities? It seems to us that these difficulties are related to the following underlying problems.

The simplicity of the fundamental Hohenberg-Kohn existence statement in no way implies a simple or obvious explicit relationship between density features and chemical properties. In fact, actual calculations of molecular energies from

molecular electron densities alone have so far proved abortive and Teller and Balasz [26] have shown that chemical bonding cannot be explained by any theory which is based on the local density alone, excluding its derivatives. Indeed, all current "density functional" calculations which have turned out to be chemically useful employ not only the local electron density, which is the object of the present inquiry, but in addition use the non-local (off-diagonal) parts of the density kernel for the evaluation of the kinetic energy. This experience reveals that the determination of the kinetic energy from the local density alone, even though possible in principle, is exceedingly difficult in practice.

The kinetic energy plays however an essential role for the covalent binding process. The often invoked electrostatic explanation, as e.g. expressed by the statement: "The resulting concentrated cloud of negative charge in the overlap region acts as a kind of electrostatic cement that holds the nuclei together... chemical bonding is mainly an effect of the additional attractive forces between the nuclei due to the overlap clouds" [27], is a much too simplistic conjecture. It has been known for two decades [10] that, in fact, covalent binding results from a *shift in the dynamic equilibrium* of the electronic motion when bonds are formed. In this context, it is also instructive that, even in classical mechanics, a nondynamic, purely static equilibrium cannot exist between electrical charges, as was shown by Earnshaw many years ago [28].

The problems with the Hellman-Feynman theorem, finally, stem from the fact that it relates densities only to forces [6b]. Binding *energies* are however of considerably greater interest than interatomic *forces* and, for a given internuclear distance, the relation between the internuclear force and the interatomic energy is not at all transparent. It is not even qualitatively unique. For example, a vanishing force does not necessarily imply the existence of a chemical bond, because the force also vanishes for metastable states, where the energy is higher than that of the separated atoms, and also at the top of energy barriers between reactants and products. Moreover, forces are proportional to r^{-2} and therefore weigh the core regions much more heavily [15] than the energy which is proportional to r^{-1}. By contrast, chemical binding can actually be fairly well described by pseudo-potential methods which completely suppress the core effects! Finally, since according to the Hellmann-Feynman theorem density behind the nuclei yields repulsive force contributions, there is no simple explanation for the accumulation of charge in the lone pair regions from this point of view.

In view of the aforementioned obstacles it is to be expected that non-trivial analyses will be needed to extract chemical information from molecular densities.

Recently, Bader et al. and Cremer and Kraka [6a] have proposed a novel complementary approach. These authors examined the first and second derivatives of the total molecular density and were able to identify charge modulations in bond, lone pair and other regions.

In our opinion the route via difference densities is close to chemical thinking and therefore deserves serious attention. The quantitative analyses presented in this investigation are meant to shed light on the opaque relationships between

chemical interactions and the details of difference density contours. It appears that many of their intricate details can be understood and related to energy changes through a decomposition and, moreover, that the natural orbitals of the density operator offer a unique and conceptually simple vehicle to this end. It is our hope that, with the help of appropriate models within this framework, it may be possible to conceptually synthesize prototype patterns for total difference densities and that the recognition of such patterns may prove useful for characterizing chemical situations. In the subsequent section we summarize the inferences we draw from the systems which we have considered.

6.2. Characteristics of difference densities

Total difference densities. States of free atoms are not spherically symmetric but they belong to irreducible representations of the three-dimensional rotation-reflection group. Consequently, densities of degenerate atomic states, such as the ^2P groundstate of fluorine, are not necessarily spherically symmetric monopoles, but quadrupolar (or possibly hexadekupolar) distributions. No contradiction exists between this statement and the observation that the response of a free atom to any measurement exhibits spherical symmetry because, in the absence of other interactions, the atom will instantly align itself with the experimental probe regardless of the directional approach. When embedded in a molecule or crystal, on the other hand, the interatomic directional forces cause orientations of the atomic building blocks relative to each other whose stability is much stronger than the interactions with, say, probing X-rays. Such atomic orientations therefore show up in density determinations by X-ray diffraction and the corresponding density quadrupoles are strikingly exhibited on those DD maps which are formed by subtracting spherically averaged atomic reference densities. We believe that these atomic orientations represent significant experimental information and that the appropriate definition and determination of such orientations is an important objective. We shall discuss a practical approach to its solution elsewhere [22].

Although the orientation of a free atom in a degenerate state requires no expenditure of energy, the concomitant density changes are often an order of magnitude larger than the density deformations that are associated with interatomic chemical interactions. In order to exhibit significant features of the latter it is therefore necessary to construct *Chemical Difference Densities* (CDDs) by subtracting, from the molecular densities, appropriately defined *oriented* atomic promolecule densities [22]. Indeed the analysis of any theoretically calculated molecular wavefunction automatically yields specific oriented atomic states for any given molecule [29]. Furthermore, the disappointing experiences which have been made with the conventional "experimental" difference densities, obtained by the subtraction of sphericalized promolecules, confirm that this arbitrary approach does not lend itself very well to an illuminating bonding analysis. We conclude that, for such analyses to be successful, the aforementioned chemical difference densities are indispensable.

The interpretation of CDDs is relatively straightforward when there are only a few interacting valence electrons. For electron-rich molecules a decomposition

into meaningful contributions from electronic subsystems seems to us essential, if one wishes to gain a deeper understanding of the various features of CDD's. We have found decompositions in terms of MCSCF (FORS) natural orbitals (NO's) to be effective and instructive. We confirm the observations of others [6b] that canonical SCF orbitals are unsatisfactory in this context. Conceivably *non-canonical* SCF-MO's could be defined which yield more meaningful decompositions of the SCF approximation to the CDD. A reasonable approach may be to construct those orthogonal SCF MO's which have maximum overlap with appropriate linear combinations of densities of the SCF AO's of the free atoms.

The characteristic pattern of a natural orbital contribution to the CDD depends upon the bond length, specifically whether the internuclear distance is to be considered as short, medium or long *for the particular natural orbital.* These distinctions are based on the value of the overlap integral between the dominant AO's from which the NO is built. A "medium" bondlength corresponds to an AO overlap integral of about 0.3–0.6. For a bonding orbital, the "normal" equilibrium distance tends to fall into this range when other valence electron interactions are absent. Overlap integrals of much less than 0.3 define "long" distances, overlap integrals much larger than 0.6 define "short" distances. It is quite possible that a particular internuclear distance counts as short for one NO, as medium for another NO and as long for a third NO in the same molecule. In such cases the various contributions have different characteristic patterns whose superposition can give a rather complex appearance to the total CDD.

Clearly, greatest insight is obtained by following up all NO contributions in a molecule separately as functions of the internuclear distance. Unfortunately, only within the theoretical approach is it possible to do so. The experimentalist is usually limited to measuring *total* densities at *equilibrium* distances. The only hope we can hold out at this time is that, on the basis of a sufficient volume of theoretical analyses, one will be able to deduce typical and well understood patterns for those difference density maps which are experimentally accessible.

Orbital difference density contributions. At *large* internuclear distances the nuclear coulomb field is still well shielded and the kinetic energy density has not changed much. Here interactions between atoms arise from electron correlation effects which reduce the interelectronic coulombic repulsion energy. Such correlations can be suitably described by valence-bond type approaches. Configuration interaction is especially important for quasidegenerate open-shell atoms. Examples are the π-π^* manifold in systems with double bonds and the d-shells in transition metal atoms. In such cases there can exist significant energetic effects while the one-electron densities undergo only small changes so that the CDD map contains little information. An example is the π-contribution for the elongated N_2 molecule, as shown in Fig. 11H.

At *medium* internuclear distances there occurs an interference between the contributing atomic orbitals which yields significant changes in the one-electron density. Concomittantly there result changes in the kinetic energy density which are essentially responsible for the substantive variations of the molecular energy

in this range. Constructive interference, accumulating charge in the bond, is associated with covalent bonding whereas destructive interference, pushing charge away from the bond region, is associated with non-bonded repulsions. These density changes can however be modified by orbital polarization and orbital contraction. They are moreover characteristically influenced by the shape of the effective potential, by the type of quasidegeneracy in the valence shell and by the orbital symmetry.

At *short* internuclear distances interference between atomic orbitals decreases and, in addition, the atoms become increasingly deshielded. Consequently, nuclear coulombic repulsions and, to some degree, core-core repulsions dominate the interatomic energy. Under the influence of the strong nuclear attractions the electron density contracts but, in doing so, it must stay outside the occupied cores [30].

The range of intermediate internuclear distances is the most interesting one and deserves a more detailed discussion. While interference is the major density changing effect towards the long end of this range, in the middle and especially towards the short end one must also take into account the "variational response" to the kinetic-energy-density change. When interference *lowers* the kinetic energy (typical bonding case), then the variational response consists of a density contraction towards the minima of the effective potentials. When an *increase* of the kinetic energy through destructive interference occurs between lone pairs with non-bonded repulsions, the response is weaker because of the greater rigidity of completely filled orbitals, but there can still occur density contractions. The shapes and magnitudes of the additional density changes resulting from the variational response depend on the shapes of the effective potentials, on the polarizability (s-p mixing) of the subsystems, on the symmetry of the dominant AO's in the particular NO, and on the presence of other valence electrons in possibly excluding orbitals.

In the case of most σ *bonding* contributions, the overlap region is the place where the kinetic energy density is low and where, at the same time, the effective potential is low. Consequently interference as well as the variational response favor charge accumulation in the bond. However this is not always so. For example, at short distances between big cores (see e.g. lower left of Fig. 2) the charge density is pushed away from the bond axis, and at large distances between small and strongly electronegative cores, where there is an effective potential maximum at the bond center (see, e.g. top right of Fig. 2), the variational response is directed towards the rim of the atomic cores (see Fig. 4E). The H_2 molecule is an extreme case of this type. Thus, a small population in a σ bond can be indicative of several situations: a long bond with small overlap; small cores of strongly electronegative atoms generating an effective potential with a maximum in the bond center (see Figs. 5A and 11E); or the close approach of large weakly attracting cores (see Fig. 3B).

In general the contributions from π *bonds* are markedly weaker than those from σ bonds (see Figs. 8 and 11). Although a π-bond is characterized by charge

accumulation in a torus around the bond axis (see Fig. 11D), an oblate total DD population does not necessarily imply π-bonding. The repulsive effect of occupied cores, when they approach sufficiently close, can squeeze the σ bond population away from the bond axis (see Figs. 3 and 11). Even in N_2 with two π-bonds, the latter are only partially responsible for the positive DD off the bond axis. Similarly, in Li_2 the σ^2-π^2 configuration mixing is only partially responsible for the oblate bond charge in Fig. 3B, C.

Charge depletions in the overlap region, which are typical for contributions from lone pairs between which there exist *non-bonded repulsions* are observed in He_2 (Fig. 1F, G), F_2 (Fig. 5B, 8B) and N_2 (Fig. 11B, F). In these cases the effective potential has a maximum in the bond center. However, when the effective potential is flat in the bond, then there can exist variational deformation responses (similar to those for bonding contributions) which compensate or possibly overcompensate the aforementioned charge depletions. For example, in Be_2 we find a density increase in the molecular center (see Figs. 2 and 3D, E). (This "bond charge" is thus not directly related to the fact that, for $R > 4a$, electron correlation cancels the non-bonded repulsions). In the hydrogen bond OH···O′ it is found [31] that the non-bonded repulsion between the bond pair in OH and the lone pair on O′ causes a charge depletion in the long hydrogen bond H···O′, where the effective potential is comparatively high, and a charge accumulation in the OH bond region where the potential is lower. The non-bonded repulsion is overcompensated by the electrostatic attraction, yielding the hydrogen bond. In the F_2 molecule the non-bonded σ lone pairs exhibit the simple charge depletion in the bond (see Figs. 5B, 8B), but a different pattern is displayed by the π-lone pair contributions. Although non-bonding, they show a slight density increase around the bond center (Figs. 5D, 8D) with a maximum at about 0.3 Å off the molecular axis where the effective p-potential is flatter than on the axis (see Fig. 2).

A special kind of non-bonded repulsion is that between the inner core of one atom and the valence orbitals on other atoms. Although its energetic effect is comparatively small, it often gives rise to a noticeable feature of DD maps, namely a dipolar pattern close to the nucleus which arises from the orthogonalization of the valence orbitals of other atoms to the core orbital [15].

In view of the many varied electronic interactions that come into play in molding the total density, the intricate details of total DD's should not be surprising. We are gratified that there appear to exist decompositions into subsystems whose contributions can be explained on the basis of well-documented energetic reasoning so that the origin of total density patterns can be better understood.

6.3. Experimental implications

The results obtained here lead to a suggestion regarding experimental practices. If the differences between the densities of oriented and those of spherically averaged atoms can be as large as those shown in Fig. 6, namely up to four electron/Å^3, then questions arise concerning the refinement of X-ray structure factors by using form factors from spherically averaged atoms only. In general,

the systematic features of residual difference densities result from two contributions: those due to orientations of nonspherical atoms and those due to binding and antibinding interactions. Of these, the former are conceptually considerably simpler than the latter. In cases where, as in F_2, the former are moreover substantially larger than the latter, it would seem advantageous to include the atomic orientations in the refinement process.

If the thermal vibration tensors are based on neutron or high-order X-ray data, then the large quadrupolar density contributions which are possible for atoms with open valence shells will result in comparatively large R-values. In such cases, it should be easily possible to determine the valence shell quadrupole tensors of those atoms and simultaneously reduce the R-factor significantly. On the other hand, if low-order X-ray data are included in the determination of the thermal smearing parameters, then the nonsphericity of an atom will modify the thermal parameters, especially their anisotropy and anharmonicity. In such cases, more reliable thermal parameters should be obtained if both, the thermal tensors and the valence shell orientations are refined simultaneously, because the former more strongly influence high-angle scattering, whereas the latter more strongly influence low-angle scattering. In many cases the valence shell asymmetry can be guessed at on the basis of simple molecular-orbital or ligand-field arguments.

While accounting for the atomic asymmetries in the refinement process should lead to more reliable thermal parameters, it will not improve atomic positions. This is so because atomic densities do not have dipolar distributions and hence cannot account for the smaller chemical deformations of dipolar type [15].

Acknowledgements. The authors are grateful to R. Ahlrichs, J. D. Dunitz, R. Goddard, E. Kraka and W. v. Niessen for constructive criticisms of the manuscript. W. H. E. Schwarz wishes to express his thanks for the cordial hospitality he experienced during his stays at the Ames Laboratory-USDOE. This work has also been supported by a NATO Research Grant (contract no. 289/83) and by Fonds der Chemischen Industrie, Frankfurt, West Germany.

References

1. Bonse, U. (ed.): Thirteenth International Congress of Crystallography, Collected Abstracts, Hamburg. Acta Cryst. A **40**, Suppl. C (1984)
2. Breitenstein, M., Dannöhl, H., Meyer, H., Schweig, A., Seeger, R., Seeger, U., Zittlau, W.: Int. Rev. Phys. Chem. **3**, 335 (1983)
3. Coppens, P., Hall, M. B. (eds.): Electron distributions and the chemical bond. Plenum Press: New York 1982
4. Becker, P. (ed.): Electron and magnetization densities in molecules and crystals. NATO-ASI-SERIES B 48. Plenum Press: New York 1980
5. Coppens, P., Stevens, E. D.: Adv. Quantum Chem. **10**, 1 (1977)

6a. An alternative approach has been proposed by Bader et al. See Bader, R. F. W., Nguyen-Dang, T. T.: Adv. Quantum Chem. **14**, 63 (1981); Cremer, D., Kraka, E.: Croat. Chem. Acta **57**, 1265 (1984)

6b. Deb, B. M. (ed.): The force concept in chemistry. van Nostrand-Reinhold: New York 1981

7a. Ruedenberg, K., Sundberg, K. R.: In: Calais, J. L., Goscinski, O., Linderberg, J., Öhrn, Y. (eds.) Quantum Science, p. 505. Plenum Press: New York 1976; Cheung, L. M., Sundberg, K. R., Ruedenberg, K.: Int. J. Quantum Chem. **16**, 1103 (1979); Ruedenberg, K., Schmidt, M. W.,

Gilbert, M. M., Elbert, S. T.: Chem. Phys. **71**, 41 (1982); **71**, 51 (1982); **71**, 65 (1982). The FORS approach is related to the CASSCF approach by Roos, Siegbahn and coworkers, see ref. 7b

7b. Siegbahn, P. E. M., Heiberg, A., Roos, B. O., Levy, B.: Physica Scripta **21**, 323 (1980); Roos, B. O., Taylor, P. R., Siegbahn, P. E. M.: Chem. Phys. **48**, 157 (1980); Roos, B. O.: Int. J. Quantum Chem. **14**, 175 (1980); Siegbahn, P. E. M., Almlöf, J., Heiberg, A., Roos, B. O.: J. Chem. Phys. **74**, 2384 (1981)

8. Schmidt, M. W., Ruedenberg, K.: J. Chem. Phys. **71**, 3951 (1979)

9. See, for instance, Bader, R. F. W., Chandra, A. K.: Can. J. Chem. **46**, 953 (1968). Note that the density difference curves for H_2 given there in Fig. 3 are incorrect, whereas the contour plots (Fig. 2) are correct

10. Ruedenberg, K.: Rev. Mod. Phys. **34**, 326 (1962) and in: Chalvet, O. et al. (eds.): Localization and delocalization in quantum chemistry, Vol. I, p. 223, Reidel: Dordrecht 1975, and other references given there. See also Kutzelnigg, W.: Angew. Chem. Int. Ed. **12**, 546 (1973)

11. Wilson, C. W., Goddard, W. A.: Theoret. Chim. Acta **26**, 195, 211 (1972)

12. Kutzelnigg, W., Schwarz, W. H. E.: Phys. Rev. A **26**, 2361 (1982)

13. Bitter, T.: Dissertation, University of Siegen 1982; Bitter, T., Ruedenberg, K., Schwarz, W. H. E.: in preparation

14. Gillespie, R. J., Nyholm, R. S.: Quart. Rev. **9**, 339 (1957). A comprehensive exposition is given in the book "Molecular Geometry" by R. J. Gillespie (Van Nostrand-Reinhold: London 1972)

15. In the immediate neighborhood of the nuclei the theoretical DD usually has a dipolar appearance because of the molecular asymmetry. While this feature has little effect on the energy (it is related to the non-bonded repulsion between the inner shell and the other atoms), it dominates the calculation of interatomic forces. Recently it has been possible to verify this characteristic experimentally by imposing the requirements of the Hellmann-Feynman theorem (balance of forces at the equilibrium geometry) on the density: Hirshfeld, F. L.: Acta Cryst. **B40**, 613 (1984). It would be of interest to apply Hirshfeld's technique to H atoms, where it can be expected to improve the X-ray determination of the atomic coordinates

16. Schwarz, W. H. E.: Theoret. Chim. Acta, **11**, 307 (1968); Chang, T. C., Habitz, P., Pittel, B., Schwarz, W. H. E.: Theoret. Chim. Acta. **34**, 263 (1974); Chang, T. C., Habitz, P., Schwarz, W. H. E.: Theoret. Chim. Acta **44**, 61 (1977)

17. Lengsfield, B. H., McLean, A. D., Yoshimine, M., Liu, B.: J. Chem. Phys. **79**, 1891 (1983); Bondybey, V. E., English, J. H.: J. Chem. Phys. **80**, 568 (1984)

18. Bader, R. F. W., Henneker, W. H., Cade, P. E.: J. Chem. Phys. **46**, 3341 (1967)

19. Blomberg, M. R. A., Siegbahn, P. E. M.: Chem. Phys. Lett. **81**, 4 (1981)

20. Smith, V. H.: p. 3 of Reference 3 and the references given therein

21. See, for instance: Dunitz, J. D., Seiler, P.: J. Am. Chem. Soc. **105**, 7056 (1983); Dunitz, J. D., Schweizer, W. B., Seiler, P.: Helv. Chim. Acta **66**, 123 (1983); see also Cremer, D., Kraka, E.: Angew. Chem. (int. edn.) **23**, 627 (1984)

22. Mensching, L., VonNiessen, W., Valtazanos, P., Schwarz, W. H. E., Ruedenberg, K.: to be published

23. See, for instance: Sanderson, R. T.: Polar covalence. Academic Press: New York 1983

24. Hohenberg, P., Kohn, W.: Phys. Rev. **B136**, 864 (1964)

25. Hellman, H.: Z. Physik **85**, 180 (1933); Acta Physiocochimica URSS **1**, 333 (1934), and Quantenchemie. Deuticke: Leipzig 1937, p. 285; Feynman, R. P.: Phys. Rev. **56**, 340 (1939)

26. Teller, E.: Rev. Mod. Phys. **34**, 627 (1962); Balasz, N. L.: Phys. Rev. **156**, 42 (1967)

27. Dewar, M. J. S.: The molecular orbital theory of organic chemistry, p. 119. McGraw-Hill: New York 1969

28. See *e.g.*: Jeans, J.: The mathematical theory of electricity and magnetism (5th edn.) p. 167. Cambridge Univ. Press 1946

29. See, for example: Lam, B., Schmidt, M. W., Ruedenberg, K.: J. Phys. Chem. **89**, 2221 (1985); Schmidt, M. W., Lam, B., Elbert, S. T., Ruedenberg, K.: Theor. Chim. Acta **68**, 69 (1985)

30. In heteroatomic molecules the electron-nuclear attraction is a driving term also at intermediate distances, causing charge transfer and contributing to ionic bonding

31. Yamable, S., Morokuma, K.: J. Am. Chem. Soc. **97**, 4458 (1975); Hermansson, K.: Acta Univ. Uppsal. **744** (1984)

32. The DD obtained from sphericalized atoms is negative on the bond path; furthermore the Laplacian of the total density is positive at the bond center, as in the case of He_2. Both were taken as evidence that the interaction in F_2 is of the closed-shell type (Bader, R. F. W., Essén, H.: J. Chem. Phys. **80**, 1943 (1984)), or that densities are not sufficient for explaining chemical bonds (Cremer and Kraka [21]). Whereas the latter conclusion is obviously correct, it supports our view that CDDs from oriented atoms are more useful than DDs from sphericalized atoms or than total densities.